Computer Methods and Programs in Biomedicine 242 (2023) 107860

Contents lists available at ScienceDirect

Computer Methods and Programs in Biomedicine

journal homepage: www.elsevier.com/locate/cmpb

Combining pharmacokinetic and electrophysiological models for early prediction of drug-induced arrhythmogenicity

Jordi Llopis-Lorente [a], Samuel Baroudi [b], Kévin Koloskoff [b], Maria Teresa Mora [a], Matthieu Basset [b], Lucía Romero [a], Sylvain Benito [b], Frederic Dayan [b], Javier Saiz [a], Beatriz Trenor [a,*]

[a] Centro de Investigación e Innovación en Bioingeniería (Ci²B), Universitat Politècnica de València, camino de Vera, s/n, 46022, Valencia, Spain
[b] ExactCure, 06000, Nice, France

ARTICLE INFO

Keywords:
Pharmacokinetic modeling
Torsade de Pointes
Cardiac safety
Population of models
Sex-specific cardiotoxicity

ABSTRACT

Background and Objective: In silico methods are gaining attention for predicting drug-induced Torsade de Pointes (TdP) in different stages of drug development. However, many computational models tended not to account for inter-individual response variability due to demographic covariates, such as sex, or physiologic covariates, such as renal function, which may be crucial when predicting TdP. This study aims to compare the effects of drugs in male and female populations with normal and impaired renal function using *in silico* methods.

Methods: Pharmacokinetic models considering sex and renal function as covariates were implemented from data published in pharmacokinetic studies. Drug effects were simulated using an electrophysiologically calibrated population of cellular models of 300 males and 300 females. The population of models was built by modifying the endocardial action potential model published by O'Hara et al. (2011) according to the experimentally measured gene expression levels of 12 ion channels.

Results: Fifteen pharmacokinetic models for CiPA drugs were implemented and validated in this study. Eight pharmacokinetic models included the effect of renal function and four the effect of sex. The mean difference in action potential duration (APD) between male and female populations was 24.9 ms ($p<0.05$). Our simulations indicated that women with impaired renal function were particularly susceptible to drug-induced arrhythmias, whereas healthy men were less prone to TdP. Differences between patient groups were more pronounced for high TdP-risk drugs. The proposed *in silico* tool also revealed that individuals with impaired renal function, electrophysiologically simulated with hyperkalemia (extracellular potassium concentration $[K^+]_o = 7$ mM) exhibited less pronounced APD prolongation than individuals with normal potassium levels. The pharmacokinetic/electrophysiological framework was used to determine the maximum safe dose of dofetilide in different patient groups. As a proof of concept, 3D simulations were also run for dofetilide obtaining QT prolongation in accordance with previously reported clinical values.

Conclusions: This study presents a novel methodology that combines pharmacokinetic and electrophysiological models to incorporate the effects of sex and renal function into *in silico* drug simulations and highlights their impact on TdP-risk assessment. Furthermore, it may also help inform maximum dose regimens that ensure TdP-related safety in a specific sub-population of patients.

Abbreviations: AP, action potential; APDx, action potential duration at x% of the repolarization; BCL, basic length cycle; CiPA, Comprehensive In Vitro Proarrhythmia Assay; Cmax, maximum concentration of a drug; Cu, unbound plasma concentration; EAD, early after depolarization; ECG, electrocardiogram; EFTPC, effective free therapeutic plasma concentration; EMw, electromechanical window; EP, electrophysiological; GFR, glomerular filtration rate; IC_{50}, half-maximal inhibitory concentration; PK, pharmacokinetic; RA, repolarization abnormality; TdP, Torsade de Pointes.

* Corresponding author.
E-mail address: btrenor@eln.upv.es (B. Trenor).

https://doi.org/10.1016/j.cmpb.2023.107860
Received 30 May 2023; Received in revised form 28 September 2023; Accepted 10 October 2023
Available online 11 October 2023

1. Introduction

Drug-arrhythmogenicity, and specifically Torsade de Pointes (TdP), is a significant concern in drug development and clinical practice [1,2]. TdP is a rare but dangerous and feared adverse drug reaction. It consists of a characteristic change in the amplitude and twisting of the QRS complex on the electrocardiogram and can cause death [3]. Drug-induced TdP has led to the withdrawal of multiple compounds from the market, including antiarrhythmics, antidepressants, painkillers, and antihistamines, among others [4]. In fact, TdP has been the most frequently reported post-approval cardiac adverse event [5]. Therefore, the assessment of drug-induced TdP is an essential aspect of drug development.

In recent years, novel approaches have been suggested for evaluating the risk of drug-induced TdP with the objective of enhancing existing regulatory directives [6]. Thus, a new cardiac safety paradigm, the Comprehensive In Vitro Proarrhythmia Assay (CiPA), was proposed in 2013 by a Think Tank supported by the Cardiac Safety Research Consortium (CSRC), the Health and Environmental Sciences Institute (HESI), and the US Food and Drug Administration (FDA) [7]. One of the pillars of CiPA is the promotion of *in silico* simulations of drug effects to improve arrhythmogenicity prediction.

In silico methods have been shown to improve and accelerate the prediction of drug-induced TdP risks, mainly in the early stages of drug development [8–12]. However, most mathematical and biophysical cardiac models based on *in silico* studies are generally developed to depict the average behavior of a group of cells characterized experimentally, ignoring inter-individual variability and predisposing factors for TdP [13]. It seems essential to consider inter-individual variability to take into account the high variation of drug responses to achieve safer drug treatments. In a recent study, we demonstrated that taking into account electrophysiological (EP) variability improves the *in silico* assessment of drug-induced torsadogenic risk [14].

In addition to EP variability, the prolongation of QT interval and subsequent TdP arrhythmia is highly influenced by many predisposing factors, such as female sex, bradycardia, heart failure, hypokalemia, or advanced age [15]. Indeed, female sex is a recognized and classical risk factor for TdP [16,17]; nevertheless, it is often underrepresented in both basic research [18] and clinical studies [19] involved in the drug development process. As an example, in the two landmark dofetilide clinical trials, DIAMOND CHF [20] and DIAMOND MI [21] trials, only 28 % of the enrolled patients were women, and in the SAFIRE-D trial [22], women accounted for only 16 % of the patients.

Another common limitation of TdP-risk *in silico* assessment tools is that most predictions are based on a single free plasma concentration of drugs extracted from the literature [8,10,12,23–25,11]. However, many factors can influence drug exposure, such as age, sex, genetics, body weight, drug interactions, and comorbidities such as renal failure [26,27]. By using pharmacokinetics (PK) modeling, it is possible to take these factors into account and predict more personalized exposure levels leading to a better overall prediction of individual risk of TdP. For example, renal failure is crucial, as it can significantly influence drug elimination [26,27]. Renal impairment is characterized by a decrease in the glomerular filtration rate (GFR) and a subsequent increase in the half-life of drugs that are eliminated by the kidneys. This can result in drug accumulation, which may lead to toxic levels and an increased risk of TdP [28]. Sex differences may also lead to significant modifications in drug distribution, metabolism and excretion [29].

This study aims to analyze the effects of sex and renal function into *in silico* drug simulations and highlights the importance of combining PK and EP models for the early prediction of drug-induced arrhythmogenicity. PK models considering sex and renal function as covariates were implemented for 15 CiPA drugs and their effects were simulated in a population of 300 male and 300 female EP models. As a proof of concept, 3D simulations of dofetilide were run to analyze modifications on the electrocardiogram (ECG). The modeling framework presented here may help in the understanding and prediction of drug PK and drug safety and is a useful tool for the evaluation of the maximum dose regimens that ensure TdP-related safety in a specific sub-population of patients.

2. Materials and methods

2.1. Drug selection

A list of 19 drugs was established based on the work of CiPA, which evaluated and categorized the potential to generate TdP of 28 molecules (cf. **Supplementary Material, Table S1**). The preliminary work of CiPA aims to provide molecules to train, test, and validate *in silico* models and cover a broad spectrum of mechanisms of action that can cause TdP [7]. This list encompasses different pharmacological classes with well-defined cardiac electrophysiology and known TdP-risk. In this work, we focused on simulating the effects of six high TdP-risk CiPA drugs (azimilide, bepridil, dofetilide, ibutilide, vandetanib, quinidine, disopyramide, and sotalol) and nine intermediate TdP-risk CiPA drugs (astemizole, chlorpromazine, cisapride, clarithromycin, clozapine, droperidol, domperidone, ondansetron, pimozide, risperidone, and terfenadine).

2.2. Pharmacokinetic models

A literature review was performed in 2021 and 2022 to select articles to implement predictive models for the selected 19 drugs. These models can be of two types: population pharmacokinetics (popPK) models or models implemented with non-compartmental data. PopPK models are nonlinear mixed effect models whose kinetic parameters values, together with characteristics (also termed covariates) effects are estimated from a dataset using dedicated pharmacometric algorithms and software. The dataset contains patient covariates to be studied, posologies and exposure time series provided at some specific sample times. Thanks to popPK models it is possible to have access to an explanation of the kinetic parameters interindividual variability in terms of selected covariates (e.g., demographic, genetic, environmental data, etc.). On the other hand, models implemented from non-compartmental analysis are based on the inference of kinetic parameter using exposure profile descriptors (e.g., area under the curve, half-life of elimination, peak concentration, and time).

The choice to implement a popPK model or a model based on non-compartmental data depended on several criteria. Initially, a popPK model is always preferred: for each molecule, a literature review was conducted to identify one or more popPK models. These models were subsequently compared and evaluated to choose the most suitable model that aligned with our requirements, using the following criteria: the general population is well represented in the model training dataset, with an important number of patients, samples, and low relative standard error. Also, for the model evaluation, the goodness of fit plots, bootstrap, and/or visual predictive checks should not reveal any bias or misspecification.

When a popPK model met the earlier criteria, it was implemented using parameters directly provided within the article and underwent validation process. If no popPK model was satisfying for a given drug, a new model was calibrated from non-compartmental data using standard non-compartmental analysis. Such approach makes it possible to manage the effect of covariates [30]. Molecules for which no model met the validation requirement were not included in the study. All models were assembled and calibrated using a dedicated modeling library developed by ExactCure company.

2.2.1. Validation criteria of pharmacokinetic models

The reference validation method for validating PK models involves the use of an external validation dataset, enabling the calculation of median prediction error (MDPE) and median absolute prediction error (MDAPE) validation criteria, used to quantify bias and inaccuracy,

respectively. To be acceptable, MDPE must be between −20 % and 20 %, and MDAPE ≤ 30 %. This method is applicable to molecules subject to clinical therapeutic drug monitoring, and a dataset is not always available. In cases where this method is not applicable, due to lack of data or absence of therapeutic drug monitoring for a drug, we are implementing a simpler validation methodology, using therapeutic thresholds.

This methodology was performed by assessing the correspondence of model simulation outputs with therapeutic thresholds from the pharmacological literature, to assess the PK behavior regarding efficacy and overexposure thresholds. Thresholds implemented are efficacy threshold (the plasma concentration at which the drug is effective) and overexposure threshold (the threshold beyond which there is no further benefit in increasing the doses) and/or toxic threshold (the threshold at which manifestations of toxicity may appear). No toxicity is expected between overexposure threshold and toxicity threshold, except if hidden toxicity occurs at this level. It is relevant to note that the meaning of the toxicity threshold may not necessarily correspond to cardiac toxicity evaluated in this paper. It could involve other types of adverse events.

This methodology allows comparing the concentration / time series obtained through model simulations to validated reference values used in clinical practice. Validating the model by using this method ensures that the concentration will fall within a therapeutic range at recommended doses by regulatory agencies. We generated various simulations to cover all the dosing regimens recommended by regulatory authorities for the various patients concerned by the treatment, by modulating the implemented covariates and recommended dosages. Outputs must be within therapeutic – overexposure or toxicity threshold to be validated.

Clozapine PK model underwent validation with an external dataset, as described by colleagues in Lereclus et al. [31]. All other models were validated using thresholds method. The thresholds used for validation are available for each drug in **Supplementary Material S2 Concentration_Time.xlsx.**

2.2.2. Covariates

Selected models include different covariates associated with plasma concentration depending on the drug. These variables encompass sex, renal and hepatic status, weight, age, cytochrome phenotypes, tobacco and alcohol consumption, among others. The covariates included in each of the fifteen PK models are available in **Supplementary Material S2 Concentration_Time.xlsx**.

As mentioned before, this study aimed to systematically investigate the effects of sex and renal function on TdP-risk; therefore, all other covariates were fixed to their respective mean population values. A weight of 70 kg was used in all simulations. In addition, to ensure consistency and homogeneity across all PK models, the continuous covariate GFR was turned into a categorical covariate called “renal function” associated to specific GFR values: normal renal function (associated to a GFR of 90 mL/min/1.73 m^2), and impaired renal function (associated to a GFR equal to 30 mL/min/1.73 m^2). In summary, two categorical covariates were considered in the PK models, resulting in four possible simulation scenarios: a) male with normal renal function; b) female with normal renal function; c) male with impaired renal function; and d) female with impaired renal function.

It is worth noting that in cases where a drug had multiple routes of administration, this study focused on the route of administration that caused the highest plasma peak concentration, as it constitutes the scenario most likely to cause TdP.

2.3. In silico populations of electrophysiological models

The EP characteristics of human ventricular cells were simulated taking as reference a modified version of the widely used human endocardial ventricular action potential (AP) model by O’Hara et al. [32]. The modifications applied to the O’Hara et al. model are described in previous studies [10,33–35]. In short, model modifications include the modulation of six ionic currents (I_{Kr} multiplied by a factor of 1.119, I_{Ks} by 1.648, I_{K1} by 1.414, I_{CaL} by 1.018, I_{NaL} by 2.274, and I_{Na} by 0.4) and a reformulation of the activation and inactivation gates of I_{Na}. These modifications were designed to better reproduce experimental data on drug effects and propagation of the electrical activity in cardiac tissue.

To account for EP variability and sex differences, we built a population of male and female EP models. To generate the male and female populations, we first obtained sex-specific normal distributions of mRNA channel expression based on the mean and standard deviations of experimentally measured gene expression levels for a set ion channels [36]. The ion channels considered were I_{Kr}, I_{Ks}, I_{K1}, I_{NCX}, I_{Na}, I_{CaL}, I_{to}, I_{pCa}, I_{NaKa}, I_{Kb}, and I_{up}. We also modified the maximum calmodulin concentration. From these gene expression distributions, we generated 50,000 sets of possible channel expression levels for males and 50,000 sets of possible channel expression levels values for females. Each set of values comprised 12 channel mRNA values, one for each of the channels considered, which were randomly sampled from the generated mRNA distributions. As a result, the generated models exhibited variability consistent with experimental observations. Gene expression values were then translated into ionic currents scaling factors by expressing them relative to mean mRNA levels of endocardial cells, as described by Yang et al. [37]. Differences in EP properties due to hormonal levels were reproduced by modifying I_{Kr}, I_{Ks}, and I_{CaL} according to Yang and colleagues [37,38]. Next, all models in the populations were simulated under control conditions (no drugs) for 500 beats. Male population was simulated with a dihydrotestosterone concentration of 35 nM, reflecting the normal high ranges in post-pubescent pre-senescent males [38]. This scenario was simulated by modifying I_{Kr} and I_{Ks} by a scale factor of 1.4 and 0.82, respectively. Female population was simulated during the early follicular phase since susceptibility to arrhythmias increases during this stage [38]. To simulate this condition, I_{Kr} and I_{Ks} were scaled by 0.86 and 1.19, respectively. Simulations were run at 37 °C and at the following extracellular concentrations: $[Na^+]_o = 140$ nM, $[Ca^{2+}]_o = 1.8$ nM and $[K^+]_o = 5.4$ nM to replicate the experimental conditions of the in vitro experiments.

After running these simulations, models with EP properties, i.e., biomarkers that did not fulfill all the calibration requirements were discarded. Plausible EP properties were defined according to the acceptable ranges found in the literature for fifteen characteristics related to AP duration, amplitude of membrane potential, and calcium

Table 1
Action potential and Ca^{2+} biomarker ranges used to calibrate the control population of human ventricular AP *in silico* models. Adapted from [14] with the two conditions for midmyocardial and epicardial cells. APDx: action potential duration at x% of the repolarization; Tri90–40: triangulation 90–40; dV/dt derivative of the voltage with respect to time; Vpeak: peak voltage; RMP: resting membrane potential; CTDx: calcium transient duration at x%; Ca^{2+} syst/diast: systolic/diastolic intracellular calcium concentration; Na^+: sodium intracellular concentration; ΔAPD90 under x% I_x: variation in APD90 under x% inhibition of I_x current.

Biomarker	Min Value	Max Value
APD40 (ms)	85	320
APD50 (ms)	110	350
APD90 (ms) (endocardial cells)	180	440
APD90 (ms) (mid-myocardial cells) [32]	350	440
APD90 (ms) (epicardial cells) [32]	240	340
Tri90-40 (ms)	50	150
dV/dt (mV/ms)	150	1000
Vpeak (mV)	10	55
RMP (mV)	−95	−80
CTD50 (ms)	120	420
CTD90 (ms)	220	785
Ca^{2+} syst. (μM)	0.262	2.23
Ca^{2+} diast. (μM)	–	0.40
Na^+ (mM)	–	39.27
ΔAPD90 (%) under 90 % IKs	−54.4	62
ΔAPD90 (%) under 70 % IKr	32.25	91.94
ΔAPD90 (%) under 50 % IK1	−5.26	14.86

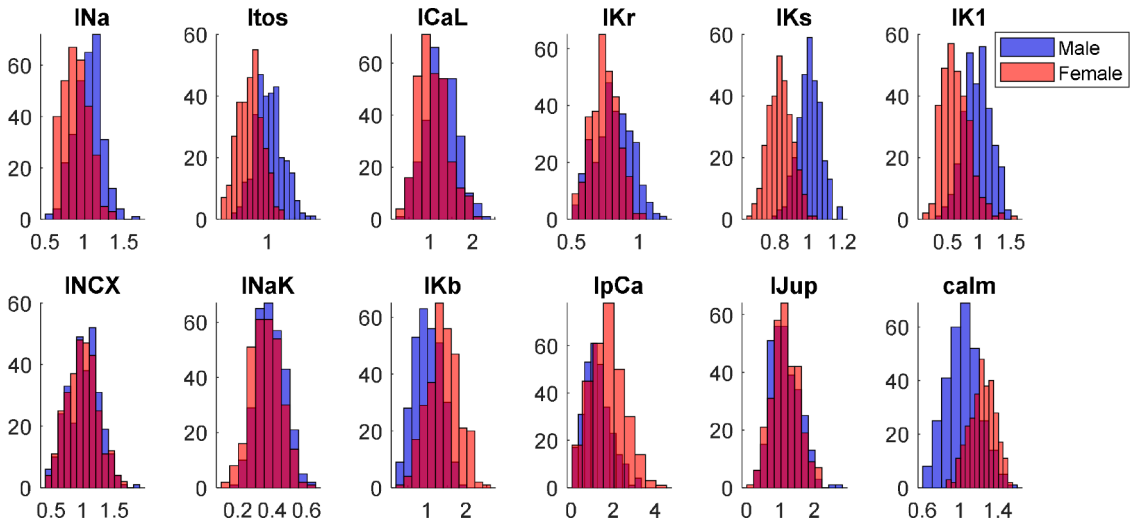

Fig. 1. Histograms of the scaling factors for the different ionic currents of the selected individuals (300 males and 300 females). Male population is represented in blue and female population is represented in red. Dark red is due to the overlap between the two groups.

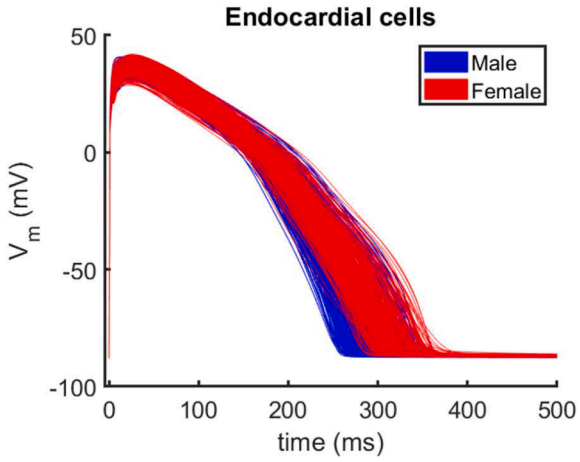

Fig. 2. Endocardial action potential traces of the male and female populations. Male population is represented in blue and female population is represented in red. Female population shows APD90s, on average, 24.9 ms longer than male (p-value<0.05).

dynamics [14]. The limits of acceptance for the fifteen biomarkers are listed in Table 1.

The populations of models were generated using MATLAB version R2022a. The source code is available at https://riunet.upv.es/handle/10251/193255.

Once calibration was performed, 300 male and 300 female models were randomly selected from the pool of models that were not discarded to further simulate drug effects. Sampling was performed using the Matlab function *randsample()*. Histograms of the scaling factors for the different ionic currents of the selected males and females are shown in Fig. 1. Male population is represented in blue and female population is represented in red. The scaling factors for the male and female populations are available in **the Supplementary Material, Table S2**.

Endocardial action potentials of male and female populations are plotted in Fig. 2. Action potential duration at 90 % of the repolarization (APD90) of the male population is 281.3 ± 22.3 ms, and APD90 of the female population is 306.2 ± 18.6 ms. Therefore, the APD90 mean difference between populations was 24.9 ms (p-value<0.05), which is in accordance with values reported in the literature [37,39].

2.4. Drug data set and drug effect simulation

Drug effects on AP were simulated via the simple pore block model. Thus, the block produced on each current was simulated by scaling the ionic current (I_i). The scaling factors were calculated using the standard Hill equation:

$$I_{i,\ drug} = \frac{1}{1 + \left(\frac{EFTPC}{IC_{50,\ i}}\right)^{h}} \cdot I_i \tag{1}$$

where $I_{i,\ drug}$ is the ionic current of channel i in the presence of the drug, $EFTPC$ is the effective free therapeutic plasma concentration (calculation is explained below in Eq. (2)), $IC_{50,i}$ is the half-maximal dose response for that drug and current through channel i, and h is the Hill coefficient, which indicates the number of drug molecules that are assumed to be sufficient to block one ion channel.

The IC_{50} and Hill coefficients of the 15 drugs were obtained from Li et al. [12]. Regarding the simulated drug concentrations, the EFTPC was calculated for each drug and scenario from the predictions of PK models as follows:

$$EFTPC(nM) = \frac{10^6 \cdot (1 - bound\ fraction) \cdot drug\ blood\ concentration\ (mg/l)}{molecular\ weight\ (g/mol)} \tag{2}$$

The blood drug concentration considered in Eq. (2) was the maximum predicted drug plasma concentration (Cmax) in each scenario for the selected drugs, as it represents the highest risk situation for inducing TdP. The bound fraction, molecular weight, and predicted EFTPC used in the different scenarios are reported in **Supplementary Material S2 Concentration_Time.xlsx**.

All simulations were carried out with a basic cycle length (BCL) of 1000 ms and a stimulus of 1.5-fold the diastolic threshold amplitude and 0.5 ms of duration. Action potential duration at 90 % repolarization (APD90) and systolic intracellular calcium concentration (Ca^{2+} syst.) were measured after 500 beats starting from control (no drug) initial condition. Net charge throughout the AP (qNet) [40], and a surrogate for the electromechanical window (EMw), defined as CTD90-APD90 [11], were calculated for the last beat. Furthermore, APs were analyzed to identify repolarization abnormalities (RAs). A RA was defined as either: i) an early after depolarization (EAD), i.e. any event with a positive voltage gradient (dV/dt > 0 mV/ms) 100 ms after the beginning of the

AP; ii) a repolarization failure, i.e. the membrane voltage at the end of the beat being higher than resting membrane voltage (Vm > -40 mV); or iii) any event with a positive calcium transient gradient ($dCa^{2+}/dt >$ 0 nM/ms) 300 ms after the beginning of the AP. In cases where RAs occurred during the last 5 beats of the simulations, none of the biomarkers were measured.

2.5. Sensitivity analysis

To evaluate the individual impact of the PK and EP models, as well as the influence of the covariates (sex and renal function) on the final drug effect, a univariate sensitivity analysis was conducted. Thus, for each drug, all four possible scenarios considered in the PK models were rigorously tested in the male and female populations (EP models).

We also investigated the effect of experimental variability of IC_{50} values on drug-induced EP changes. Specifically, we examined the influence of experimental uncertainty on measurements of I_{Kr}/hERG inhibition potency on the final drug effect. We focused on I_{Kr} inhibition because of its strong association with TdP generation [2]. Then, for each drug, we ran simulations varying the hERG IC_{50} value considered. We used the minimum, mean, and maximum values of hERG IC_{50} estimated for each drug by Li et al. [12]. A constant drug concentration was used for all the simulations of a given drug. In particular, we simulated the EFTPC predicted by the PK model for a male with normal renal function, in the population of male EP models and in the population of female EP models.

2.6. ECG simulations

As a proof of concept to demonstrate the feasibility of our approach, we conducted dofetilide simulations in a 3D biventricular model and propagated them to an anatomically detailed human torso to obtain realistic ECG signals under the four scenarios: male with normal renal function, male with impaired renal function, female with normal renal function, and female with impaired renal function. Dofetilide was selected because of its sex- and renal status-dependent pharmacokinetics and its wide clinical usage, providing reliable validation data.

In this study, we used a 3D patient-specific biventricular *in silico* model obtained from delayed enhanced magnetic resonance images (DE-MRI) previously developed by our group [41,42]. The resulting hexahedra-based volume mesh contained 4 million nodes (vertices) and 3.71 million elements, with an average edge length of 380 μm. Transmural heterogeneity was included in the biventricular model by defining three different transmural layers for the endocardial, mid-myocardial, and epicardial cells. These layers comprised 17, 41, and 42 % of ventricular wall thickness, respectively. Longitudinal and transversal conductivities of the tissue were set to 0.24 S/m and 0.0456 S/m, respectively. Consequently, the conduction velocity measured 0.68 m/s along the fiber direction and 0.26 m/s in the transverse direction, which is consistent with experimental measurements taken in human ventricles [43]. In addition, the anisotropy of the cardiac muscle due to fiber orientation was accounted for by using a Streeter's rule-based method, as previously described [42]. The model also included a His-Purkinje System network composed of 1391 Purkinje-myocardial junctions generated through a stochastic growth method using linear elements, as detailed by our group [41,42,44].

The biventricular *in silico* model was fitted into an anatomically detailed human torso mesh to accurately solve the forward problem in electrophysiology and thus obtain realistic simulated ECGs. The torso mesh consisted of 1.26 million nodes and 7.35 million tetrahedral elements with an average edge length of 0.55 mm [41,42,44,45]. The 3D torso model included bones, lungs, liver, whole heart (ventricles and atria), and the blood pools of all cardiac chambers. For the different organs and tissues, we used the same conductivity values as Ferrer et al. (2015) [44], which were taken from the literature. To simulate the ECG signals, virtual electrodes were placed on the surface of the torso model to correspond to the standard 12 electrocardiographic leads.

At the cellular level, we selected the ID6 male model (see **Supplementary Material, Table S2**) as a representative of the male population and the ID35 female model (see **Supplementary Material, Table S2**) as a representative of the female population. Transmural heterogeneity of the myocardium was considered, as mentioned above. For Purkinje cells, we used the model published by Stewart and colleagues [46].

The electrical propagation through the ventricles was calculated by solving the monodomain equation (Eq. (3)) with ELVIRA software [47], which is based on a pseudo-adaptive finite element method in space and time to solve reaction-diffusion equations with highly nonlinear reactive terms.

$$\nabla\cdot(\mathbf{D}\nabla V_m) = C_m\frac{\partial V_m}{\partial t} + I_{ion} + I_{stim} \tag{3}$$

where **D** represents the diffusion conductivity tensor, the transmembrane potential field is denoted by V_m, the cell membrane capacitance is expressed as C_m, the transmembrane ionic current is indicated by I_{ion}, and the transmembrane stimulation current is represented by I_{stim}.

ECG was simulated by solving the extracellular potential (φ_e) using Eq. (4):

$$\nabla\cdot([D_i + D_e]\nabla\varphi_e) = -\nabla\cdot(D_i\nabla V_m) \tag{4}$$

where D_i and D_e refer to the volume-averaged conductivity tensors of the intra and extracellular domains, respectively. As in [42], the reaction-diffusion simulation was run on the biventricular mesh. The right-hand side of Eq. (4) was evaluated on this fine mesh and then interpolated on the coarse torso mesh. Further details on ECG computations are available in [42,45].

Drug simulations were run for 5 beats with a basic cycle length of 1000 ms. Stimuli with an intensity of 900 μA/μF and a duration of 2 ms were applied to the first node of the His bundle.

When determining drug effects at the whole-heart level, we measured the QT interval, as it is a prognostic biomarker for the development of TdP [3]. As described by Pokorney et al. [16], the QT interval was measured from the onset of the QRS complex to the intersection of the line of the maximal slope of the T-wave and the T-P isoelectric baseline. The QTc interval measurements were determined in the last beat in the limb lead I.

3. Results

3.1. Pharmacokinetic models for predicting plasma concentration of 15 CiPA drugs

Of the 19 molecules selected, 15 PK models were developed: six for high TdP-risk drugs (azimilide, dofetilide, vandetanib, quinidine, disopyramide, and sotalol); and nine for intermediate TdP-risk drugs (chlorpromazine, cisapride, clarithromycin, clozapine, droperidol, domperidone, pimozide, risperidone, and ondansetron). Astemizole and terfenadine could not have been implemented due to a lack of published PK data, while bepridil and ibutilide models did not meet PK model validation criteria and were not implemented.

The implemented models were one-compartment and two-compartment based on literature popPK studies, or one-compartment models implemented from non-compartmental data. The models structures, parameters and sources are summarized in Table 2.

The two types of model structures are represented in Figs. 3 and 4. These figures illustrate how the parameters for Table 2 are used to calibrate the model. For one-compartment models implemented from non-compartment data, calibration was performed by ExactCure tools using basic formulas of Pharmacokinetics [30].

Table 2
Structures, parameters, and sources of implemented PK models. This table summarizes the parameters implemented to calibrate PK models. 3 types of models were implemented: 1- and 2-compartment models implemented from popPK studies, and 1-compartment models implemented from non-compartmental data. *F*: bioavailability (no unit); *ka*: absorption rate (hours^{-1}); *CL*: clearance (liters/hour); *Vd*: distribution volume (liters); V1: volume of the central compartment (liters); *V2*: volume of the peripheral compartment (liters); *Q*: intercompartmental clearance (liters/hour); *T1/2*: half-life of elimination (hours); *Tmax*: time to reach the maximum concentration (hours); *Cmax*: maximum concentration (mg/liter); *Tlag*: lag time (hours). Covariates implemented as Boolean ("if true" = 1) were: *sex_m* (sex male), *smoker, heart failure, alcoholic, height < 175 cm, GFR (glomerular filtration rate) <50, cyp2d6 status* (cytochrome 2D6 is a major hepatic enzyme involved in drug metabolism). Covariates implemented as continuous were: *weight, GFR, age*.

One-compartment model implemented from popPK studies

Drug	F	ka (h^{-1})	Cl (L/h)	Vd (L)	Source
Azimilide	1	0.497	$3.92 \times (\text{weight} - 43)^{0.208} \times (1 + 0.171 \times \text{sex\_m}) \times (1 + 0.155 \times \text{smoker})$	$717 + 9.88 \times (\text{weight} - 43)$	[48]
Cisapride	1	2.58	If weight > 6.5 kg: 0.16635 × weight (Calculated with T1/2 = 10 h and Vd) If weight ≤ 6.5 kg: 0.538 × weight	If weight > 6.5 kg: 2.4 × weight If weight ≤ 6.5 kg: 21.9	[49–51]
Clozapine	1	$1.24 + (0.13 \times \text{sex\_m})$	$39.9 + (8 \times \text{sex\_m})$	$564 + (155 \times \text{sex\_m})$	[52]
Quinidine	1	0.894	$(18 - 0.101 \times \text{Age}) \times (1 + 0.156 \times \text{height} < 175\text{ cm}) \times (1 - 0.115 \times \text{heartfailure}) \times (1 + 0.230 \times \text{alcoholic}) \times (1 - 0.178 \times \text{GFR} < 50)$	230	[53]

Two-compartment model implemented from popPK studies

Drug	F	Ka (h^{-1})	V1 (L)	Cl (L/h)	V2 (L)	Q (L/h)	Source
Droperidol	1	10	73.6	41.9	79.8	71.5	[54]
Pimozide	1 Tlag: 1.14 h	0.68	1240	54.9 × (1 + (cyp2d6_poor x (−0.3624))) × (1 + (cyp2d6_intermediate × (−0.7322)))	1040	69.2	[55]
Risperidone	1 Tlag: 0.235 h	2.39	$137 \times \frac{weight}{70}$	$(4.66 \times \frac{weight^{0.75}}{70} + 0.00831 \times \text{glomerular\_filtration\_rate}) \times \frac{weight^{-0.172}}{70}$	$86.8 \times \frac{weight}{70}$	1.35	[56]

One-compartment model implemented with non-compartmental data

Drug	F	T1/2 (h)	Tmax (hours)	Vd (L)	Cmax (mg/L)	Source
Clarithromycin	0.55	3.8	1.7	3 × weight	–	[57]
Chlorpromazine	0.32	30	2.5	$1470 \times \frac{weight}{70}$	–	[58]
D, L Sotalol	0.8	7.18	3.1	84.7	–	[58]
Disopyramide	0.95	6.3	Immediate Release: 1.5 Extended Release: 4.5	0.75 × weight	–	[59,60]
Dofetilide	0.9	10	2.5	3 × weight	–	[61]
Domperidone	0.831	8	Tablet: 1.2 Oral solution: 0.9	–	Tablet : 0.0396 Oral solution : 0.043	[62]
Ondansetron	0.55	3	1.9	140	–	[63]
Vandetanib	1	195.4	6	$3876 \times \frac{weight}{80.7}$		[64]

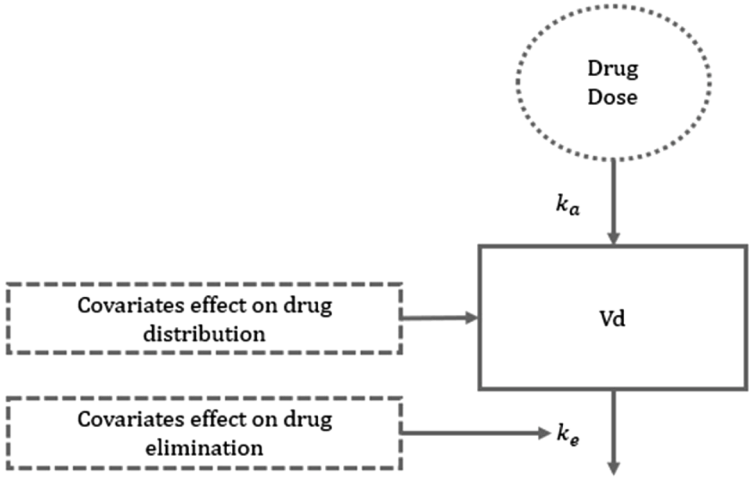

$$\frac{dx1}{dt} = ka \cdot xa - ke \cdot x1$$
$$\frac{CL}{Vd} = ke$$

Fig. 3. 1-compartment model general structure. *x1*: quantity in central compartment (mg); *xa*: quantity in the theoretical absorption compartment (mg); *ka*: absorption rate (hours^{-1}); *Vd*: distribution volume (L); *ke*: elimination rate (hours^{-1}). Covariates effects could impact absorption, distribution, elimination.

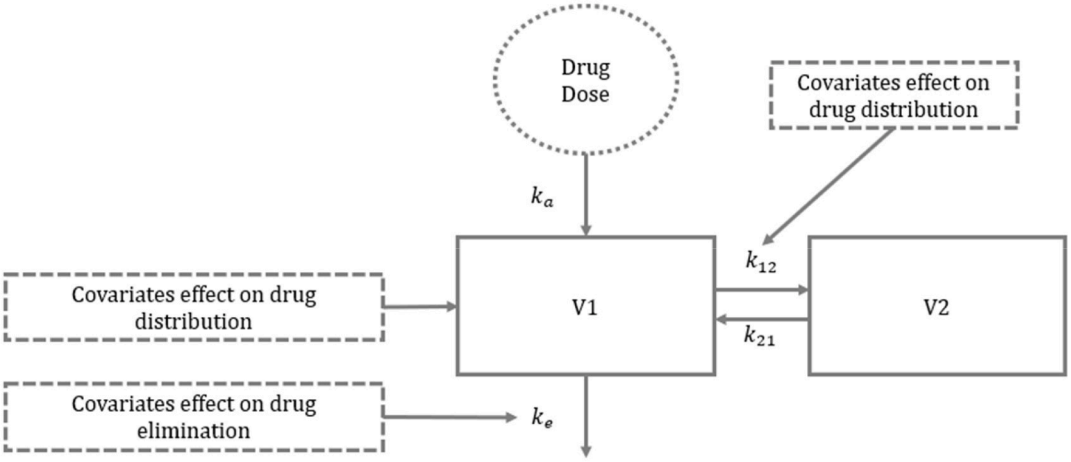

$$\frac{dx1}{dt} = ka \cdot xa + k_{21} \cdot x2 - ke \cdot x1 - k_{12} \cdot x1$$

$$\frac{dx2}{dt} = k_{12} \cdot x1 - k_{21} \cdot x2$$

$$\frac{CL}{Vd} = ke$$

$$\frac{Q}{V1} = k_{12}$$

$$\frac{Q}{V2} = k_{21}$$

Fig. 4. 2-compartment model general structure. *x1*: quantity in central compartment (mg); *x2*: quantity in the peripheral compartment; *xa*: quantity in the theoretical absorption compartment (mg); *ka*: absorption rate (hours^{-1}); *V1*: volume of the central compartment (L); *V2*: volume of the peripheral compartment (L); *ke*: elimination rate (hours^{-1}); k_{12} *and* k_{21}: intercompartmental transfer constant (hours^{-1}). Covariates effects could impact absorption, distribution, elimination.

3.1.1. *Pharmacokinetic models validation*

The validation process for the 15 implemented PK models was performed successfully. Clozapine PK model was validated using an external database in Lereclus et al. [31]. Dataset contained 151 samples from 53 patients, MDPE was −19 % and MDAPE was 29.4 %, showing absence of bias and inaccuracy.

The other 14 PK models were evaluated using the therapeutic thresholds method. Models' outputs were evaluated regarding selected therapeutic thresholds from the literature. The tests assessed whether simulations with the parameters of the dosages recommended by the health authorities, as well as the patients concerned by these dosages (whose profiles were created by modulating the values of the covariates) were within the therapeutic threshold. Concentration over time series and the thresholds used to perform the validation are available for each drug in **Supplementary Material S2 Concentration_Time.xlsx.**

3.1.2. *Covariates*

As previously noted, this study specifically examined the influence of sex and renal function. Eight models included the effect of renal function, and four models the effect of sex (see **Supplementary Material S2 Concentration_Time.xlsx**). Moreover, PK models allow the simulation of temporal changes in blood concentrations with different dosing regimens.

Different scenarios were simulated for each drug, depending on the implemented covariates in the PK models and recommended dosing regimens according to the summary of product characteristics. All simulated drug plasma concentrations are available in the **Supplementary Material S2 Concentration_Time.xlsx**.

Fig. 5 shows as an example the time course of free plasma concentration for 2 high TdP-risk drugs (dofetilide and quinidine) and 2 intermediate TdP-risk drugs (clarithromycin and clozapine) as a function of sex and renal function. The simulated dosing regimens for each drug were established according to the recommended dose for a standard healthy individual and are indicated in the respective summary of product characteristics: 0.5 mg/12 h (oral) for dofetilide, 600 mg/8 h (oral) for quinidine, 450 mg/12 h (oral) for clozapine, 500 mg/12 h (intravenous) for clarithromycin. Plasma levels of dofetilide are highly influenced by renal function, as evidenced by a significant increase in blood concentration in a male with impaired renal function compared to a male with normal renal function. Specifically, the blood concentration of dofetilide in a male with impaired renal function was approximately threefold higher than in a male with normal renal function. Moreover, sex-related differences in dofetilide concentrations were also observed, particularly in individuals with renal impairment. In contrast, quinidine and clarithromycin only exhibit differences in blood concentration based on renal function and not sex. Furthermore, renal impairment has a greater impact on the pharmacokinetics of clarithromycin compared to quinidine, since the differences between normal and impaired renal function are significantly higher in clarithromycin. On the other hand, for clozapine, the differences in blood concentration are solely due to sex, with no significant impact of impaired renal function on drug levels. Regarding the remaining eleven drugs, it can be observed that for disopyramide, sotalol, and vandetanib (high TdP-risk drugs), renal status significantly influences drug levels. In contrast, azimilide (high TdP-risk drug) only exhibits slight differences between males and females, and drug levels are independent of renal status. As for the other seven intermediate TdP-risk drugs, renal function only appears as a covariate in two drugs (chlorpromazine and domperidone), and in general, sex produces minimal differences (observations that can be extracted from **the Supplementary Material S2 Concentration_Time.xlsx**).

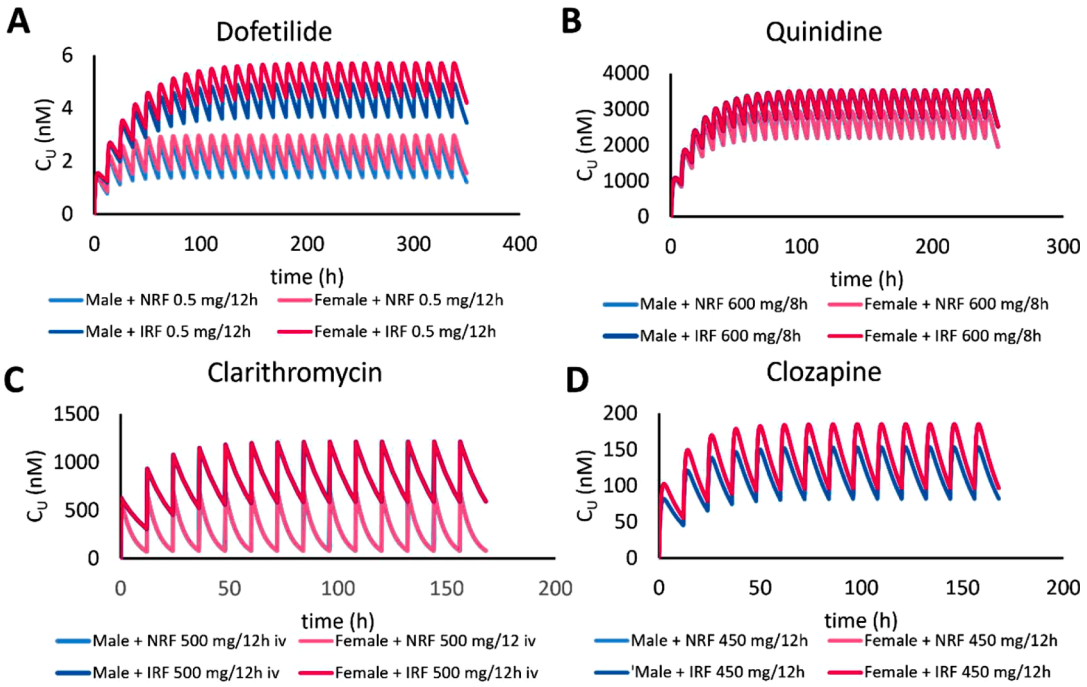

Fig. 5. Time-evolution of unbound plasma concentrations (C_U) of 2 high TdP-risk drugs – dofetilide and quinidine – (A&B) and 2 intermediate TdP-risk drugs – clarithromycin and clozapine – (C&D) depending on different characteristics of the patients (sex and renal function). NRF: normal renal function. IRF: impaired renal function.

3.2. Drug effects at the cellular level

After obtaining the predicted blood concentrations of the fifteen drugs in the four studied scenarios, the simple pore block model was used to determine the effect of each drug on the different ion currents. Fig. 6 shows the effects of the concentrations predicted by the PK models of dofetilide, quinidine, clarithromycin, and clozapine on I_{Kr} using the EFTPC obtained from PK models. I_{Kr} block has traditionally been recognized as the primary cause associated with the onset of TdP [2], thus increased inhibition of I_{Kr} is correlated with a higher likelihood of TdP occurrence (assuming all other currents remain unchanged). Notably, the high TdP-risk drugs examined in this study exhibited a pronounced blockade of I_{Kr}. As shown in Fig. 6, both high TdP-risk drugs produced a substantial reduction in I_{Kr}, with drug scale factors below 0.5 for the four scenarios considered. In contrast, for intermediate TdP-risk drugs, the drug scale factors for I_{Kr} are practically 100 %. Furthermore, it is noteworthy that the intermediate TdP-risk drugs show minimal or negligible differences in I_{Kr} drug scale factors between the different scenarios studied. The most significant difference is observed for dofetilide, as renal function appears to have the largest impact.

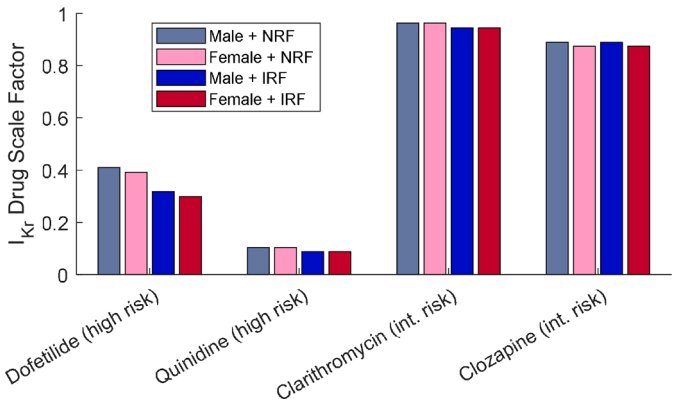

Fig. 6. Effects on I_{Kr} for the 4 different simulated scenarios of 2 high TdP-risk drugs (dofetilide and quinidine) and 2 intermediate TdP-risk drugs (clarithromycin and clozapine). NRF: normal renal function; IRF: impaired renal function.

It is remarkable that for certain drugs, important differences at the PK level between individuals may not translate into significantly different effects in the EP model. For instance, clarithromycin exhibits a nearly two-fold increase in plasma concentration due to renal function (Fig. 5); however, such changes do not propagate to a significant extent in the EP model.

This inhibition of the different ion channels translates into EP changes. Fig. 7 shows the effects of dofetilide at the cellular level for the four scenarios studied. It can be observed that among the four different scenarios studied, women with impaired renal function are the most susceptible patient group in terms of prolongation of APD and presence of RAs induced by dofetilide.

One of the most common problems experienced by patients with renal insufficiency is electrolyte imbalance. Specifically, hyperkalemia is a frequent alteration in these patients, with a prevalence of approximately 20 % [65]. Hyperkalemia manifestations usually occur when the serum potassium concentration is $\geq$ 7.0 mM with chronic hyperkalemia [66]. In order to study the combined effects of hyperkalemia and pharmacological effects, simulations were conducted with $[K^+]_o = 7.0$ mM. Fig. 8 shows the results of these simulations, combining the effects of dofetilide, renal impairment, and hyperkalemia in both the male and female populations. It can be observed that hyperkalemia partially compensates for the torsadogenic effects of dofetilide, resulting in less prolongation of APD90 and lower incidence of RAs. Under hyperkalemia conditions, the male population with renal impairment had APD90s that were, on average, 49.2 ms shorter than under normokalemic conditions. In the female population with renal impairment, hyperkalemia led to APD90s that were, on average, 54.5 ms shorter. The incidence of RAs in the male population with renal impairment decreased from 1 (normokalemia) to 0 (hyperkalemia), while in the female population with renal impairment decreased from 10 (normokalemia) to 1 (hyperkalemia). These results evidence the mitigating effect of hyperkalemia on the torsadogenicity of drugs in patients with impaired renal function.

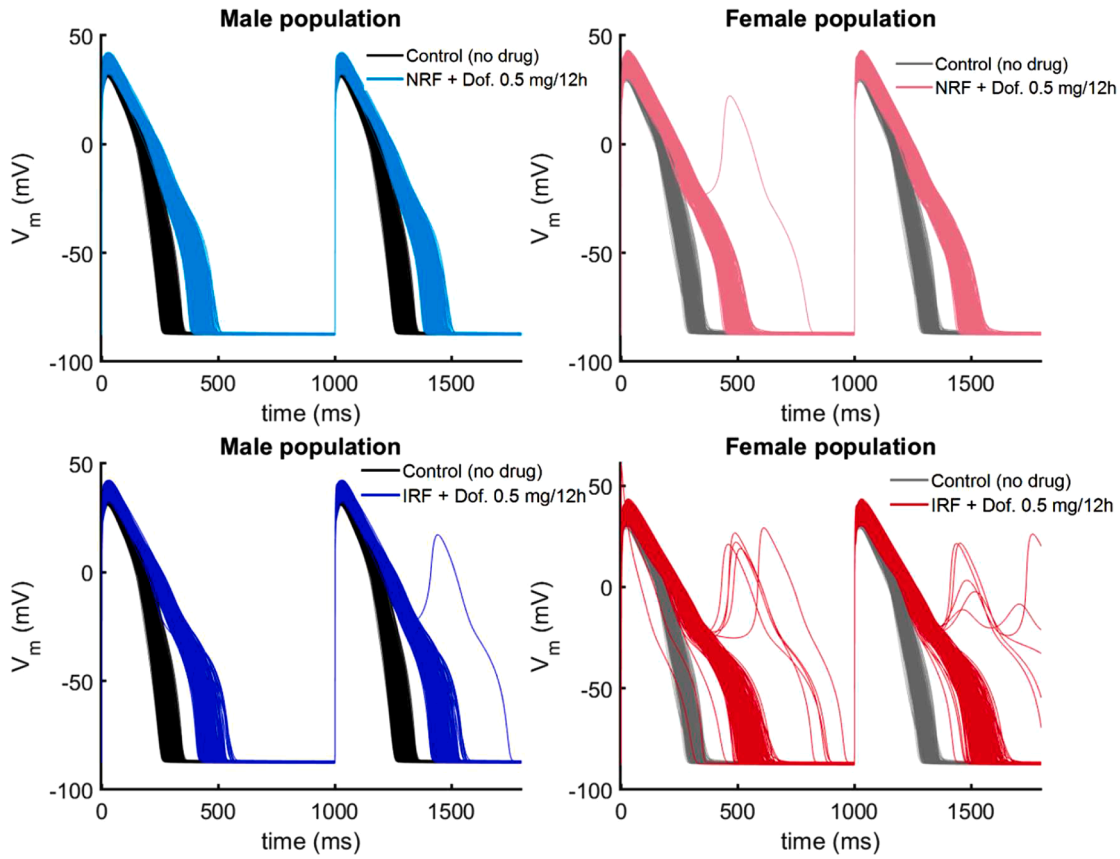

Fig. 7. Effects of dofetilide (high TdP-risk drug) at the cellular level for the four studied scenarios. NRF: normal renal function; IRF: impaired renal function; Dof.: dofetilide.

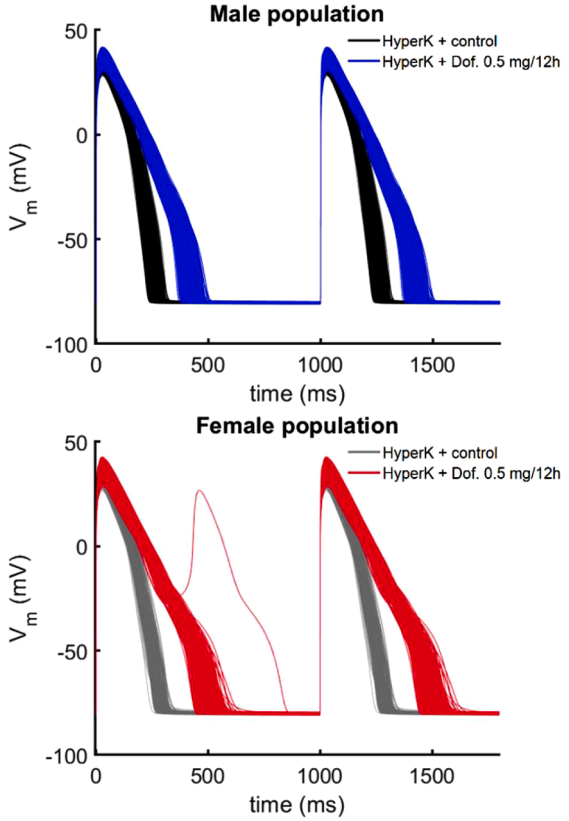

Fig. 8. Effects of dofetilide (high TdP-risk drug) at the cellular level in the male (top panel) and female (bottom panel) populations with impaired renal function and hyperkalemia ([K+]=7.0 mM). HyperK: hyperkalemia; Dof.: dofelitide.

After running simulations of the fifteen CiPA drugs in the four scenarios investigated, four biomarkers associated with the risk of TdP induction were measured: APD90, qNet, EMw, and Ca^{2+} syst. APD90 and qNet distributions in the four scenarios for the fifteen drugs studied are shown in Figs. 9 and 10, respectively. EMw and Ca^{2+} syst. distributions are shown in the **Supplemental Material, Figure S1 and Figure S2.** Our simulations confirmed that women with impaired renal function presented larger APD90s and lower values of EMw, qNet and Ca^{2+} syst. Thus, women with impaired renal function were found to be particularly susceptible to drug-induced TdP, while men with normal renal function were the sub-population who demonstrated a lower propensity to TdP. Differences between patient groups were more prominent for high TdP-risk drugs.

The drug with the highest torsadogenicity was quinidine, which caused 218 (72.7 %) RA events in the female population with renal impairment, 202 (67.3 %) RA events in the female population with normal renal function, 113 (37.7 %) RA events in the male population with renal impairment, and 94 (31.3 %) RA events in the male population with normal renal function. The other drug that caused RA events was dofetilide, with 10 (3.3 %) events in the female population with renal impairment, 1 (0.3 %) RA in the female population with normal renal function, and 1 (0.3 %) RA in the male population with impaired renal function. Intermediate TdP-risk drugs showed minimal alterations in biomarkers compared with control conditions.

3.3. Sensitivity analysis on pharmacokinetics and electrophysiological models

To assess the specific influence of the PK and EP models on the overall drug effect, univariate sensitivity analysis was performed. In this analysis, we focused on the APD90 biomarker. The results of the sensitivity analysis are shown in Fig. 11. For clarity, only the mean APD90

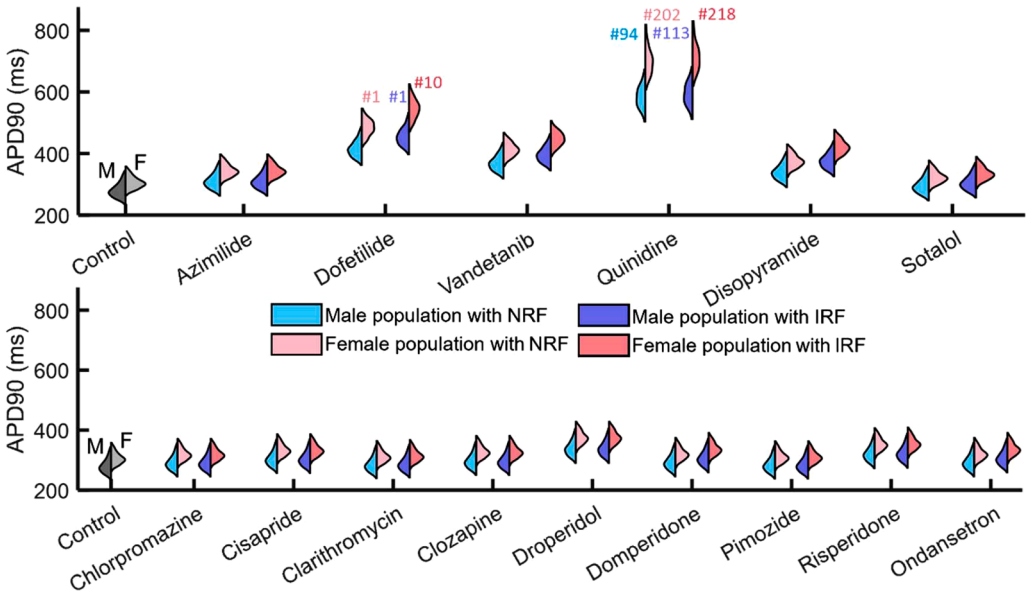

Fig. 9. Distribution of APD90 in the four scenarios under the effect of high TdP-risk drugs (top) and under the effect of intermediate TdP-risk drugs (bottom). # indicates the number of drug-induced RAs (cases in which RAs appear are not represented in the distribution). NRF: normal renal function; IRF: impaired renal function.

values of the population of 300 male and 300 female models are represented in the figure. For each drug, the red or blue line indicate the same population of EP models (red for females and blue for males); therefore, along the same line, only the simulated drug concentration changes (corresponding to the one predicted by the PK model). The four simulated scenarios with PK models are represented by points of different colors (light blue for males with normal renal function, pink for females with normal renal function, blue for males with impaired renal function, and red for females with impaired renal function). It can be observed that EP characteristics have a higher impact compared to the effects of PK features. Indeed, vertical distances between blue and red lines are more marked than vertical distances between circles in the same line. Quinidine is the drug in which the female population of EP models produced higher differences compared to the male population of EP models. Regarding PK models, renal function is the covariate that has the highest influence, particularly in the high TdP-risk drugs (Fig. 11, top panel) dofetilide, vandetanib, and disopyramide (differences between light and dark circles within the same lines). Among the intermediate TdP-risk drugs (Fig. 11, bottom panel), domperidone is the only drug for which renal status has a significant effect; for the other intermediate TdP-risk drugs, the covariates in the PK models have limited impact.

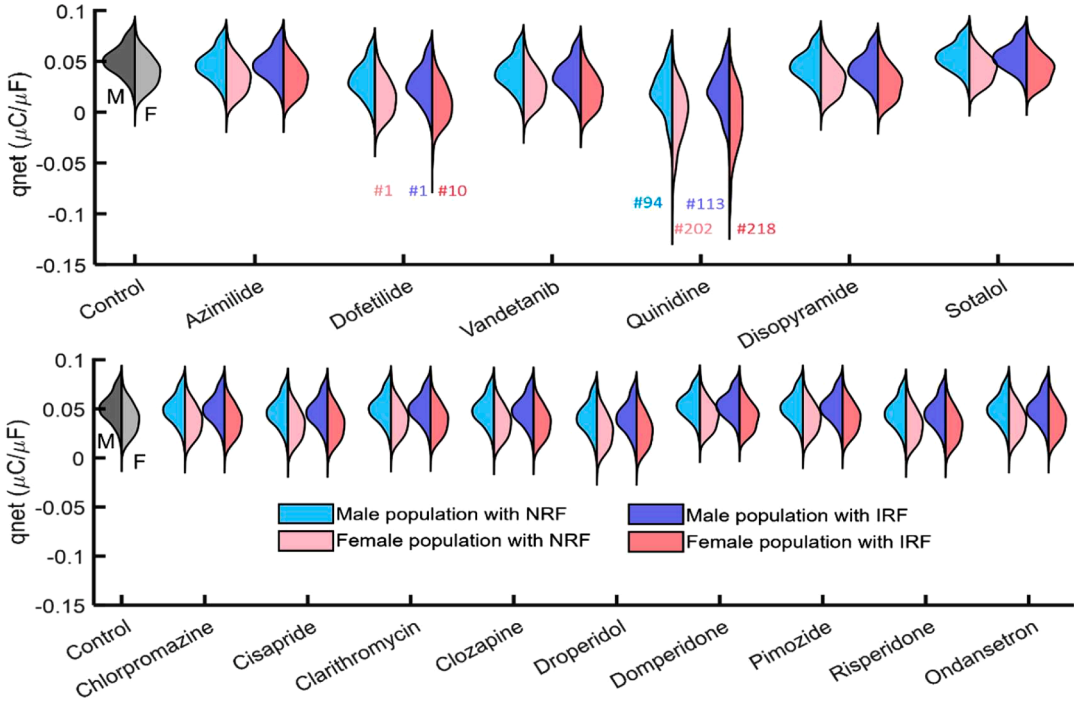

Fig. 10. Distribution of qNet in the 4 scenarios under the effect of high TdP-risk drugs (top) and under the effect of intermediate TdP-risk drugs (bottom). # indicates the number of drug-induced RAs (cases in which RAs appear are not represented in the distribution). NRF: normal renal function; IRF: impaired renal function.

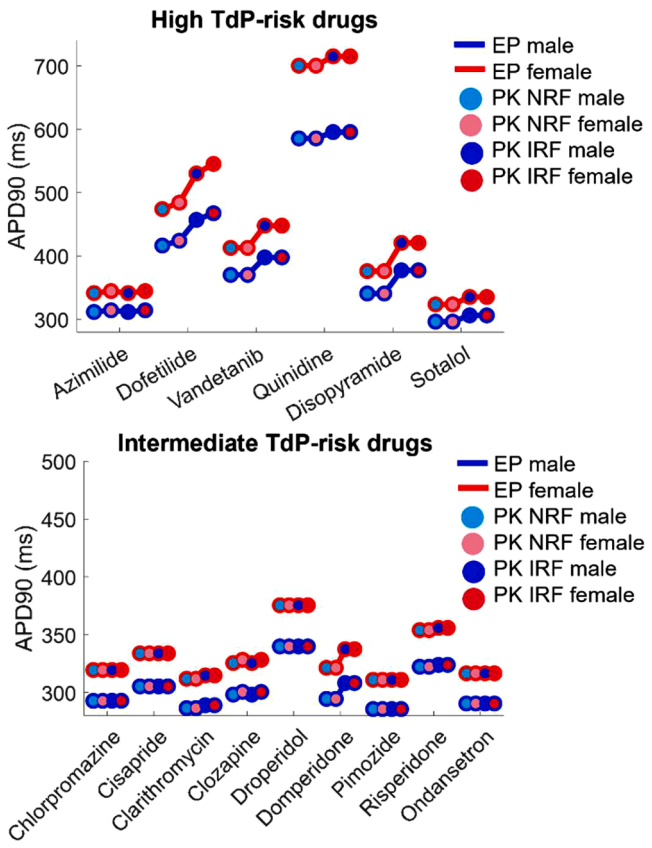

Fig. 11. Sensitivity analysis of the individual impact of the PK and EP models on the high TdP-risk drugs (top panel) and on the intermediate TdP-risk drugs (bottom panel). NRF: normal renal function; IRF: impaired renal function.

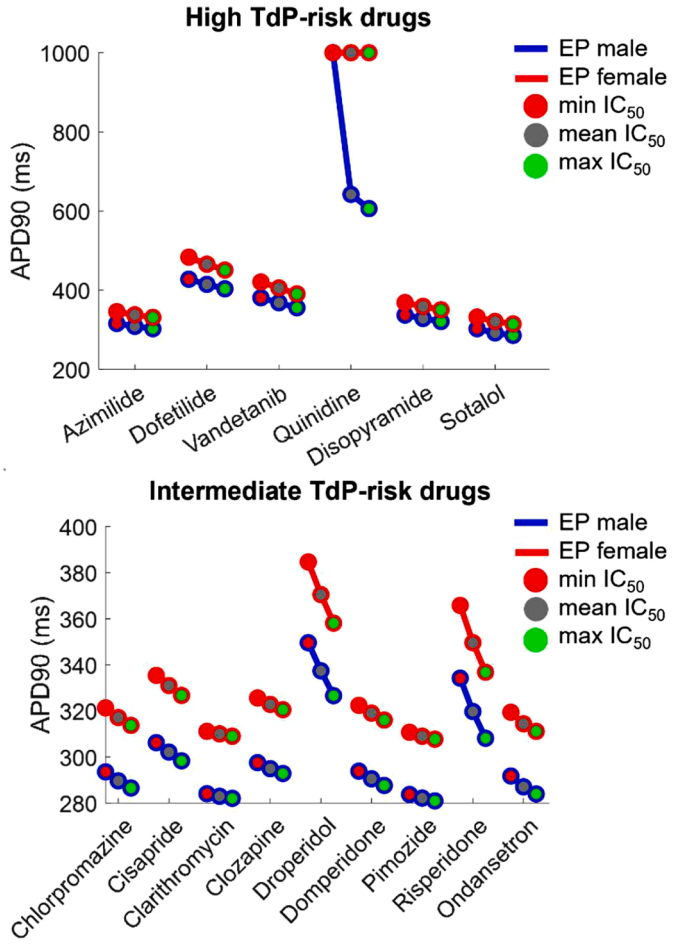

Fig. 12. Sensitivity analysis of hERG IC_{50} variability impact on the high TdP-risk drugs (top panel) and on the intermediate TdP-risk drugs (bottom panel).

3.4. Sensitivity analysis on hERG IC_{50}

A sensitivity analysis of the influence of experimental variability in hERG IC_{50} on the APD90 was also performed. This set of simulations was run using only the plasma concentration predicted for a man with normal renal function for each drug. The minimum, mean, and maximum hERG IC_{50} for values estimated by Li et al. [12] for each drug were used in this analysis. Fig. 12 shows the results of the sensitivity analysis. As shown in Fig. 11, for each drug, each line represents the same population of EP models. When RAs appeared, the APD90 value was set to 1000 ms.

Quinidine exhibits the highest sensitivity to variations in the value of hERG IC_{50}. Specifically, in the male EP model population, using the minimum IC_{50} value leads to RAs. However, in general, other drugs do not show significant differences in APD90 due to variations in hERG IC_{50}. The drugs with the most significant differences in APD90 due to changes in hERG IC_{50} are dofetilide, vandetanib, droperidol, and risperidone (note the different scale in both panels). The differences in APD90 between simulations with the minimum and maximum IC_{50} values for these drugs are 32.5 ms, 30.1 ms, 29 ms, and 26.6 ms, respectively. Conversely, for the remaining drugs, the differences in APD90 are below 20 ms.

3.5. Modification of dose regimen for sub-population with higher TdP-risk

One of the advantages of the developed PK/EP framework is its ability to efficiently test a wide range of dosing regimens in a rapid and straightforward manner and thus identify the maximum safe dose for specific sub-populations. As an example, the use case of dofetilide is presented herein. As shown in Fig. 13, the standard dosage (0.5 mg/12 h) given to the female population with impaired renal function resulted in significant prolongation of APD90 and the occurrence of RAs in 10 out of 300 models. According to the dofetilide summary of product characteristics [61], the dosage for sub-populations with a GFR between 20 – 40 ml/min/1.73 m^2 should be reduced to 0.125 mg/12 h. When simulating dofelitide effects at the readjusted posology, the incidence of RAs significantly decreased from 10/300 to 0/300. Furthermore, APD90 was also reduced from 545.95 ± 33.11 ms to 431.03 ± 22.67 ms in the simulations with the re-adjusted dosage.

3.6. ECG changes due to drug effects

As a proof of concept, we conducted 3D simulations of dofetilide in the four studied scenarios to analyze changes in the ECG. The simulations were performed using the ID6 male model and the ID35 female model. Fig. 14 shows the simulated ECG traces recorded at standard lead I.

Under control conditions, QT interval for the simulated male model was 406 ms, whereas for the simulated female model QT interval was 422 ms. When dofetilide effects were simulated in the male with normal renal function, QT interval was prolonged to 466 ms. Interestingly, in the case of the male with impaired renal function, QT interval further increased to 507 ms, suggesting a higher risk of drug-induced TdP in individuals with renal impairment.

Similarly, in the female model with normal renal function, dofetilide prolonged the QT interval to 510 ms, which could potentially predispose the heart to arrhythmic events. Notably, in the female model with impaired renal function, the administration of dofetilide resulted in the appearance of an arrhythmia. These findings highlight the importance of

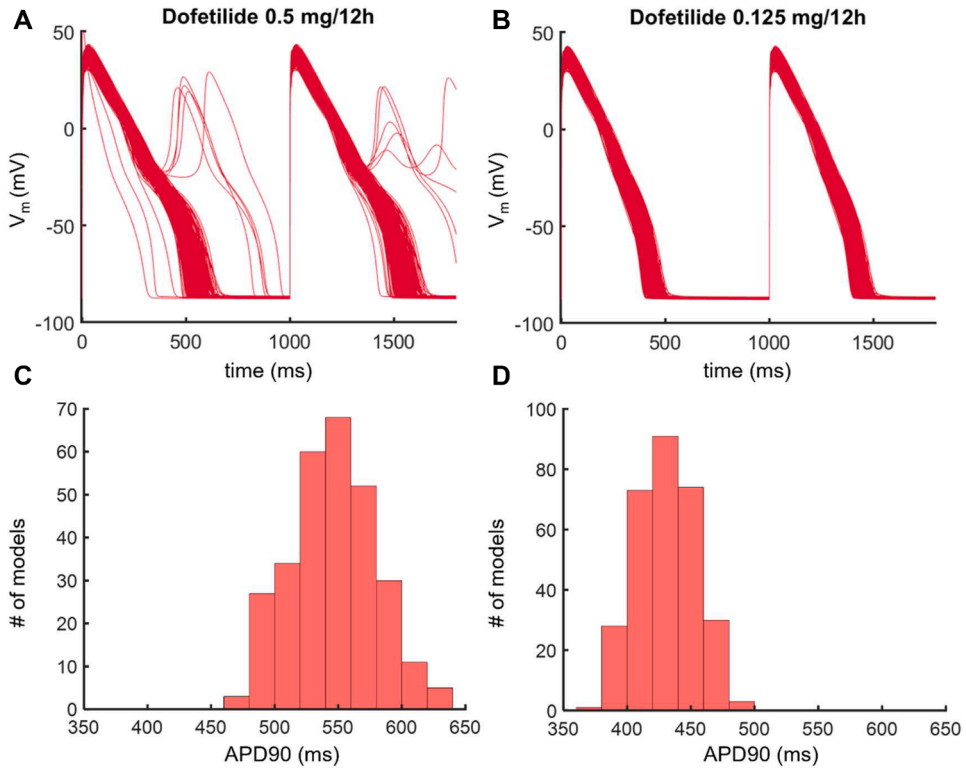

Fig. 13. Effects of dofetilide (high TdP-risk drug) in the female population with impaired renal function before (left) and after (right) dose adjustment. (A) AP traces under dofetilide effect at a standard dosage (0.5 mg/12 h). (B) AP traces under dofetilide effect after adjusting the dosage for sub-populations with TdP risk factors (0.125 mg/12 h). (C) Histogram of APD90 in the female population with impaired renal function under dofetilide effect at a standard dosage (0.5 mg/12 h). Models with RAs were not represented (10 models). (D) Histogram of APD90 in the female population with impaired renal function under dofetilide effect after dose adjustment (0.125 mg/12 h).

considering renal function and sex as crucial factors for determining drug safety.

A video showing the propagation patterns through the heart and the ECG signals can be found in **Supplementary Material S3. Propagation-ECG.mp4**

4. Discussion

4.1. Main findings

In this study, we demonstrated the benefits of combining PK and EP models for the prediction of drug-induced TdP-risk in different sub-populations. The major findings of this study are as follows:

(i) We implemented 15 PK models for CiPA drugs, identifying some covariates associated with drug plasma concentration levels and simulated a broad range of dose regimens and patient scenarios, which are available in **Supplementary Material S2 Concentration_Time.xlsx**. Eight PK models included the effect of renal status, and four models included the effect of sex as covariates.

(ii) There is a significant difference in drug effects between sub-populations. Women with impaired renal function are particularly susceptible to drug-induced arrhythmias. This emphasizes the need to consider sex and renal function as important factors when evaluating drug safety and optimizing dose regimens.

(iii) PK differences in drug concentrations do not always translate into significant modifications of the EP properties, as exemplified with clarithromycin. This suggests that the relationship between PK and EP effects may be complex, emphasizing the importance of integrating PK and EP models to comprehensively evaluate drug-induced TdP-risk.

(iv) The developed PK/EP framework enables efficient testing of a wide range of dosing regimens in different clinical scenarios, guiding the identification of the maximum safe dose and the dose adjustments needed for specific sub-populations. This was demonstrated using the example of dofetilide, where re-adjustment of the dose regimen in the female population with impaired renal function significantly reduced the incidence of RAs.

4.2. Predictions of drug plasma concentration with pharmacokinetic models

PK models can be a valuable tool during the assessment of drug-induced TdP-risk, as they allow the generation of a priori simulations. This means that PK models can be used to predict drug concentrations at different time points, under different dosing regimens, and in different patient populations. Thereby, pharmaceutical companies and regulatory agencies, such as the US Food and Drug Administration, are increasingly relying on them [67].

In this study, we implemented fifteen PK models. We simulated distinct scenarios, considering different patient characteristics, routes of administration, posologies, etc. The simulated scenarios are available in **Supplementary Material S2 Concentration_Time.xlsx**.

Among the two covariates studied here, renal function was found to have the greatest influence on drug concentrations (although fewer PK models included it as a covariate). This is consistent with previous research showing that renal function can significantly affect drugs levels [68].

The benefits of using PK models in combination with EP models for the evaluation of TdP-risk have also been previously demonstrated. Polak [69] combined PK and EP models demonstrating reliable QT predictions of quinidine and its metabolite 3-OH-quinidine effects using

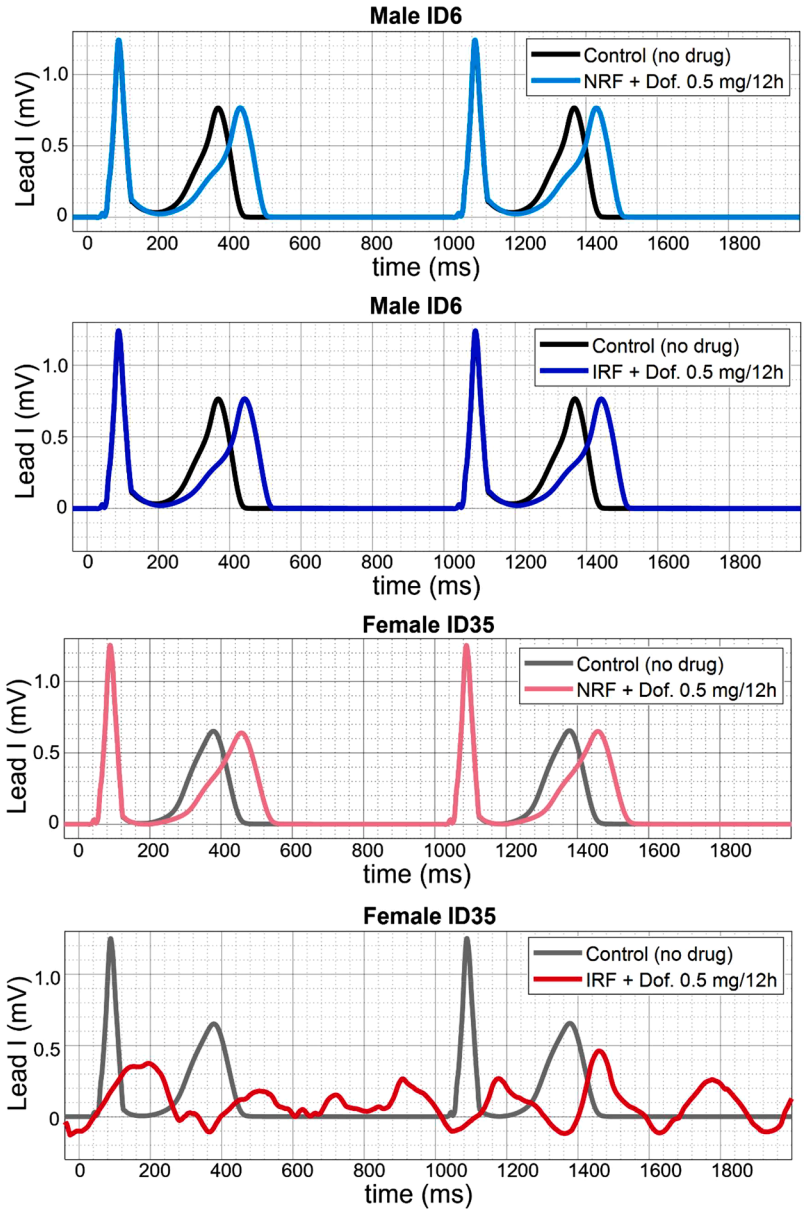

Fig. 14. ECG effects of dofetilide at a standard dosage in the four studied scenarios: male with normal renal function (top panel – light blue line); male with impaired renal function (second panel – blue line); female with normal renal function (third panel – pink line); female with impaired renal function (bottom panel – red line). Black and gray lines represent the male and female models, respectively, in control conditions. NRF: normal renal function. IRF: impaired renal function. Dof.: dofetilide.

exclusively *in vitro* data. Varshneya et al. used simulations of PKs and EP models to predict the arrhythmic risk of four drugs proposed for the treatment of COVID-19 (lopinavir, ritonavir, chloroquine, and azithromycin), demonstrating that the combination of PK and EP modeling predicts more precisely the cardiac risk of therapies [70]. Wisnowska et al. [71] used PK models to simulate the concentration-time profiles of fenspiride and analyzed its effect on EP models through pseudoECG signal modifications and the qNet metric. Zhou and colleagues [72] also showed that using PK models to predict myocyte drug concentration facilitated better TdP-risk predictions. The PK models implemented here enable the stratification of predicted exposure based on patient features, including demographic and clinical biological characteristics. As exemplified with dofetilide, this information can help guide drug development decisions, such as dose selection, dosing interval, and patient selection, with the goal of optimizing drug safety and efficacy. Further advancements in personalization could involve Bayesian parameter estimation, depending on the availability of data.

4.3. *Electrophysiological drug effects and TdP risk factors*

Here, we propose a methodology to create a population of male and female EP models based on genome-scale sex differences in cardiomyocytes [36,73] and considering hormonal effects [37,38]. Our resulting parameterizations accurately recapitulated the differences in the AP properties reported in basic research [37,39]. Furthermore, the 3D simulations ran with the representative male and female EP models as a proof of concept also reproduced the clinically described ECG properties [74–76]. For instance, the male and female simulated QT intervals (406 ms and 422 ms, respectively) fall within the range of 394 ±16 ms for males and 408±15 ms for females described by Vicente et al. [74], and the range of 405.7 ± 15.8 ms for males and 411.9 ± 14.6 ms females described by Surawicz et al. [75]. Moreover, the simulations also replicate other reported male ECG characteristics in comparison with female ECG, such as a shorter period between the J-point and the onset of the T wave, steeper slope of the ST segment, steeper ascent of

the T wave, higher T wave amplitude, and shorter and less horizontal ST segment [75].

The simulations of drug effects in our study are in line with experimental studies and previous *in silico* works [8–10,14,23,77–82]. For instance, Chen et al. [81] reported that 10 nM of sotalol produced an average APD90 prolongation of 300 ms. In our simulations, 12 μM of sotalol in the male population resulted in an average APD90 prolongation of 296.5 ms. In another study, the effect of 3 μM of clarithromycin was an APD90 prolongation of 18 ms [80]. Similarly, in our simulations, 1.2 μM of clarithromycin resulted in an APD90 prolongation of 8.8 ms in the female population. Another work showed that a concentration of 10 nM of dofetilide produced a change in APD90 of 276±56 ms [77], and in our simulations, 4.9 nM of dofetilide resulted in an APD90 prolongation of 175.7 ± 17.9 ms.

In general, it can be affirmed that high TdP-risk drugs induced more remarkable changes in the biomarkers, prolonging APD90, reducing qNet and EMw, and increasing Ca^{2+} syst., indicating a higher propensity for arrhythmias [14]. Notably, our simulations of different patient groups revealed that, compared with diseased men or healthy individuals of either sex, women with impaired renal function are particularly vulnerable to drug-induced arrhythmias. Furthermore, in the sensitivity analysis, the female sex in the EP models was found to be the covariate posing the highest risk for drug-induced TdP, even surpassing renal function. Varshenya et al. [70] also found that in their *in silico* study the number of drug-induced RAs in their healthy female population was higher than in their male population with heart failure.

Over the past two decades, it has been increasingly recognized that the female sex is a significant risk factor for TdP. Thus, some authors state that women are twice as susceptible to drug-induced arrhythmias as men [16,17,83,84]. However, the impact of sex differences on drug-induced arrhythmogenicity, particularly in the field of *in silico* studies, remains largely understudied. Very few researchers have started to introduce the effect of sex in their simulations [37,38,85–87], and the general conclusion is consistent across these studies: including sex as an independent factor in preclinical assessment of drug-induced proarrhythmic risk is crucial to prevent potentially life-threatening consequences for the female population.

Nonetheless, as demonstrated in this study, the increased TdP-risk is not solely explained by sex, but rather by a combination of other factors, such as renal impairment. This is in line with the multi-hit theory, which suggests that TdP occurs due to a combination of multiple factors, including genetic predisposition, drug-induced ion channel block, electrolyte imbalances, cardiac diseases, among others [88]. In accordance with our findings, renal impairment has been associated with an increased risk of TdP [89]. One of the advantages of the described PK/EP framework is the possibility of simulating the combined effects of several factors simultaneously. In this sense, by simulating the effects of possible hyperkalemia, our results suggest that hyperkalemia could have a potential protective role against the development of TdP. These results are consistent with the findings described by Genovesi et al. [90], who reported that patients undergoing hemodialysis had less cardiac electrical stability than those undergoing peritoneal dialysis, due to significant decreases in potassium levels. In fact, hypokalemia has been clinically associated with the occurrence of TdP [15,89].

Finally, the effects of dofetilide observed in our 3D simulations are consistent with the effects on the QT interval described for this drug in clinical trials, further validating the utility of our PK/EP framework for studying drug-induced arrhythmias. Johannesen et al. [91] conducted a prospective clinical trial involving 22 healthy individuals in which they reported that a 0.5 mg dose of dofetilide resulted in a prolongation of the QT interval by 79.3 ms (95 % confidence interval: 72.2 - 86.3 ms). Similarly, Coz's and colleagues [92], in their study of healthy volunteers, showed an average increase in the QT interval of 61 ms after taking a dose of 0.5 mg of dofetilide. In addition, our simulation of the female model with normal renal function reached a QT interval over 500 ms after taking dofetilide, which, according to the Medication Guide, indicates a need to reduce the dosage [61]. This finding is consistent with the study by Pokorney et al. [16], which reported that 55 % of the female participants who took dofetilide 0.5 mg twice daily required discontinuation or dose reduction. Moreover, our study provides further support for the recommendation of dosage reduction in cases of renal impairment [61]. In the simulated renal impairment scenarios, under the standard dofetilide dose regimen, the male model experienced excessive QT prolongation, while the female model developed TdP. These findings emphasize the importance of adjusting dosages in patients with predisposing factors to mitigate the risk of drug-induced TdP.

4.4. Limitations of the study

Despite the strengths and findings of this study, there are several limitations that should be considered when interpreting the results. One limitation is related to the IC_{50} values obtained from the literature. The reliability and accuracy of these values vary with various factors, such as different experimental conditions or methodologies, which may introduce inherent limitations and uncertainties in the study [93–95]. We attempted to mitigate this issue by performing a sensitivity analysis and by using the pharmacological data provided by Li et al. [12], aiming to reduce inter-experiment variability. Furthermore, these IC_{50} values were generated in accordance with CiPA recommendations for experimental settings.

One of the inherent constraints associated with this approach is the need for pharmacokinetic data to implement a PK model. This limitation necessitates the exclusion of certain models due to a lack of data. Regarding the introduction of new molecules to the market, it would be conceivable to establish a collaborative arrangement that includes PK modeling steps, thereby enabling the utilization of this approach.

Another limitation of our approach is the coupling of PK models with EP models through the Hill equation. PK models predict as output blood time concentration for the drug of interest, while the Hill equation takes this concentration as an input and compares it directly against in vitro IC_{50}s. This comparison of variables from different sources, each with their own uncertainties, can introduce potential conflicts. However, to address this concern, we performed a sensitivity analysis of IC_{50}s values for hERG and found that drug effect simulations were not significantly affected, providing some assurance regarding the robustness of our findings despite this limitation.

Regarding the concentrations used in this study, drug effects were simulated with EFTPC (effective free therapeutic plasma concentrations). Free drug concentration, rather than the total concentration, is often considered more relevant for therapeutic drug monitoring as only the unbound fraction can reach the site of action [96–98]. Furthermore, prior research has demonstrated that predictions derived from plasma concentration tend to yield superior electrophysiological changes predictions compared to total concentration [69]. However, it is important to recognize that free plasma concentration serves as a surrogate for tissue concentration. It is generally assumed that the unbound drug concentration within tissues is in equilibrium with the free drug concentration in the circulatory system. Nevertheless, this assumption may not be true for drugs that tend to accumulate at the tissue level (e.g., chloroquine - not simulated here - can exhibit a peak tissue/plasma concentration ratio greater than 300 [99]). In such cases, knowledge of intracellular concentration or subcellular drug distribution could further enhance the accuracy of predicting drug efficacy and toxicity. Polak et al. [100] reviewed some example of PK models including the heart compartment (and PK models for other tissue compartments). Due to the modular design of the proposed simulation framework, future works could consider the incorporation of tissue-level concentrations to refine predictions of drug effects.

An additional limitation of this work might be related to the use of mRNA channel expression levels for building the population of models. It is known that mRNA channel expression levels may not fully capture

the complexity and activity of ion channels [101]. mRNA expression is one of the many factors that determine the expression of ion channels in the cell membrane, although other factors, such as translation rate, binding with channel subunits, methylation, membrane localization, trafficking, and phosphorylation, also play important roles in regulating the activity of ion channels. Nevertheless, mRNA expression data still provides valuable information on variability in the heart [102]. Therefore, we believe that using distributions based on mRNA channel expression levels to generate the populations of EP models is advantageous compared with using synthetic distributions. In addition, it is worth noting that the presented approach for building the population of EP models assumes independence in ionic current variability. While this assumption is based on available experimental data regarding ionic current covariance, it introduces a level of uncertainty into our simulations. Additional information regarding ionic current correlations could be easily implemented into the proposed simulation framework and potentially enhance the accuracy of predictions.

Furthermore, another aspect to be considered is that there might be parameters describing sex and renal function effects which have not been considered in this work (for example heart rate differences, weight differences, cardiomyocytes volume and capacitance differences, plasma protein levels). The inclusion of additional parameters related to sex and renal function could represent an enhancement in future investigations by allowing more accurate predictions of drug effects.

On the other hand, it is important to note that this study did not analyze the effect of certain covariates that could potentially influence drug-induced TdP-risk, such as weight, smoking habits, height, age, or CYP2D6 mutations [103]. Weight was kept constant at 70 kg across the four simulated PK scenarios. This simplification may not fully replicate real-world variations, but this decision aimed at isolating the primary effects of sex. Moreover, the study primarily focused on TdP as a specific adverse drug reaction, but there may be other arrhythmogenic risks or unwanted drug effects that have not been fully assessed. Furthermore, the interactions between two or more drugs or the effect of active metabolites were not considered in the simulations. Effects of active metabolites and real-world interactions between multiple drugs in a clinical setting may be complex and could potentially affect the risk assessment and safety profile of the drugs. The absence of such interactions within the modeling framework may limit the real-world applicability of the findings. In addition, the study lacked electromechanical simulations that could provide mechanistic information regarding the detrimental hemodynamic changes associated with drug-induced effects on cardiac electrophysiology. While the focus of the study was not on electromechanical simulations, the absence of this aspect may limit the mechanistic understanding of the hemodynamic effects of drugs and their potential impacts on patient outcomes. However, the modeling framework proposed here could be combined with other tools to generate an integrative model for multi-organ drug-induced toxicity prediction. Future studies could explore additional factors and incorporate more comprehensive and mechanistic simulations to further enhance our understanding of drug-induced cardiac EP effects and their potential clinical implications.

It is important to acknowledge the limitations of this study and recognize the need for further research and validation to establish the robustness and applicability of the approach in diverse populations and clinical scenarios. Despite these limitations, this study yielded promising results and proposes a valuable methodology for *in silico* drug-induced TdP assessment.

5. Conclusions

This study demonstrates the potential of a combined PK/EP framework for improving drug TdP-risk assessment. By using PK models together with virtual sex-specific populations of EP models based on mRNA channel expression levels, this approach constitutes a more refined and quantitative approach to assess drug safety in subpopulations with higher TdP-risk. The simulations conducted provided valuable insights into the complex interactions between drug effects, sex, and renal function, identifying female sex and impaired renal function as risk factors for drug-induced TdP.

Furthermore, the proposed methodology may be useful for optimizing dose and drug regimens, potentially minimizing the cost of phase I/II clinical trials. While this study focused specifically on sex and renal function, other factors such as comorbidities (e.g., heart failure, myocardial infarction, or hepatic dysfunction), genetic polymorphisms, active metabolites effects, or drug-drug interactions could be incorporated into the proposed modeling framework to expand its utility. *In silico* medicine, as demonstrated by this study, offers the possibility of testing a wide range of factors in a systematic and efficient manner, providing quantitative and population-specific risk assessments, optimizing drug therapies, and improving patient safety in the context of drug-induced TdP. Further research in this area may contribute to the development of personalized medicine approaches, ultimately leading to safer drug therapies for patients.

Author contributions

All authors contributed to the conceptualization and design of the study. Data curation, formal analysis, validation and visualization of the results was carried out by JL, SaBa and KK. SaBa and KK constructed the PK models, simulated potential clinical scenarios, and validated the PK models, under the supervision of SyBe and FD. JL and LR generated the population of male/female EP models. JL conducted the EP simulations, curated the data, and contributed to the formal analysis. BT, LR and JS supervised the EP simulations. All the authors participated in the discussion of the results. JL wrote the first draft of the manuscript with assistance from SaBa and KK. SyBe, MT, BT, and JS reviewed and edited this draft. All authors contributed to the thorough review of the final manuscript and read and approved the submitted version.

Funding

This project received funding from the European Union's Horizon 2020 Research and Innovation Program under grant agreement No. 101016496 (SimCardioTest). This work was also partially supported by the Dirección General de Política Científica de la Generalitat Valenciana (PROMETEO/2020/043). The authors also thankfully acknowledge the computer resources at MareNostrum and the technical support provided by Barcelona Supercomputing Center (IM-2021-1-0001, IM-2021-1-0003, IM-2022-1-0002, IM-2023-1-0002). JL is being funded by the Ministerio de Ciencia, Innovación y Universidades for the Formación de Profesorado Universitario (grant reference: FPU18/01659). Funding for open access charge: Universitat Politècnica de València.

Declaration of Competing Interest

Samuel Baroudi, Kévin Koloskoff, Mathieu Basset, Sylvain Benito, and Frederic Dayan work for ExactCure®.

All the other authors declare no potential commercial or financial relationships.

Acknowledgments

The authors would like to thank Dr. Jordi Cano for his assistance in the preliminary work for the construction of the male and female population of EP models.

Supplementary materials

Supplementary material associated with this article can be found, in the online version, at doi:10.1016/j.cmpb.2023.107860.

References

[1] P.T. Sager, G. Gintant, J.R. Turner, S. Pettit, N. Stockbridge, Rechanneling the cardiac proarrhythmia safety paradigm: a meeting report from the cardiac safety research consortium, Am. Heart. J. 167 (2014) 292–300, https://doi.org/10.1016/j.ahj.2013.11.004.

[2] J. Vicente, R. Zusterzeel, L. Johannesen, J. Mason, P. Sager, V. Patel, M.K. Matta, Z. Li, J. Liu, C. Garnett, N. Stockbridge, I. Zineh, D.G. Strauss, Mechanistic model-informed proarrhythmic risk assessment of drugs: review of the "CiPA" initiative and design of a prospective clinical validation study, Clin. Pharmacol. Ther. 103 (2018) 54–66, https://doi.org/10.1002/cpt.896.

[3] M. Li, L. Ramos, Drug induced QT prolongation and torsades de pointes, Pharm. Ther. 42 (2017) 473–477. https://www.ncbi.nlm.nih.gov/pmc/articles/PMC5481298/.

[4] L. Krumpholz, B. Wiśniowska, S. Polak, Open-access database of literature derived drug-related Torsade de Pointes cases, BMC Pharmacol. Toxicol. 23 (2022) 1–4, https://doi.org/10.1186/S40360-021-00548-0.

[5] H.G. Laverty, C. Benson, E.J. Cartwright, M.J. Cross, C. Garland, T. Hammond, C. Holloway, N. McMahon, J. Milligan, B.K. Park, M. Pirmohamed, C. Pollard, J. Radford, N. Roome, P. Sager, S. Singh, T. Suter, W. Suter, A. Trafford, P.G. A. Volders, R. Wallis, R. Weaver, M. York, J.P. Valentin, How can we improve our understanding of cardiovascular safety liabilities to develop safer medicines? Br. J. Pharmacol. 163 (2011) 675–693, https://doi.org/10.1111/J.1476-5381.2011.01255.X.

[6] J.S. Park, J.Y. Jeon, J.H. Yang, M.G. Kim, Introduction to in silico model for proarrhythmic risk assessment under the CiPA initiative, Transl. Clin. Pharmacol. 27 (2019) 12–18, https://doi.org/10.12793/TCP.2019.27.1.12.

[7] T. Colatsky, B. Fermini, G. Gintant, J.B. Pierson, P. Sager, Y. Sekino, D.G. Strauss, N. Stockbridge, The comprehensive in vitro proarrhythmia assay (CiPA) initiative — update on progress, J. Pharmacol. Toxicol. Methods 81 (2016) 15–20, https://doi.org/10.1016/j.vascn.2016.06.002.

[8] Y. Yoo, A. Marcellinus, D.U. Jeong, K.-S. Kim, K.M. Lim, Assessment of drug proarrhythmicity using artificial neural networks with in silico deterministic model outputs, Front. Physiol. 0 (2021) 2289, https://doi.org/10.3389/FPHYS.2021.761691.

[9] D.U. Jeong, Y. Yoo, A. Marcellinus, K.M. Lim, D.U. Jeong, Y. Yoo, A. Marcellinus, K.M. Lim, Application of convolutional neural networks using action potential shape for in-silico proarrhythmic risk assessment, Biomedicines 11 (2023) 406, https://doi.org/10.3390/BIOMEDICINES11020406.

[10] J. Llopis-Lorente, J. Gomis-Tena, J. Cano, L. Romero, J. Saiz, B. Trenor, In silico classifiers for the assessment of drug proarrhythmicity, J. Chem. Inf. Model. 60 (2020) 5172–5187, https://doi.org/10.1021/acs.jcim.0c00201.

[11] E. Passini, C. Trovato, P. Morissette, F. Sannajust, A. Bueno-Orovio, B. Rodriguez, Drug-induced shortening of the electromechanical window is an effective biomarker for in silico prediction of clinical risk of arrhythmias, Br. J. Pharmacol. 176 (2019) 3819–3833, https://doi.org/10.1111/bph.14786.

[12] Z. Li, B.J. Ridder, X. Han, W.W. Wu, J. Sheng, P.N. Tran, M. Wu, A. Randolph, R. H. Johnstone, G.R. Mirams, Y. Kuryshev, J. Kramer, C. Wu, W.J. Crumb, D. G. Strauss, Assessment of an in silico mechanistic model for proarrhythmia risk prediction under the CiPA initiative, Clin. Pharmacol. Ther. 105 (2019) 466–475, https://doi.org/10.1002/CPT.1184.

[13] H. Ni, S. Morotti, E. Grandi, A heart for diversity: simulating variability in cardiac arrhythmia research, Front. Physiol. 9 (2018) 1–19, https://doi.org/10.3389/fphys.2018.00958.

[14] J. Llopis-Lorente, B. Trenor, J. Saiz, Considering population variability of electrophysiological models improves the in silico assessment of drug-induced torsadogenic risk, Comput. Methods Programs Biomed. 221 (2022), 106934, https://doi.org/10.1016/J.CMPB.2022.106934.

[15] K.E. Trinkley, R.L. Page, H. Lien, K. Yamanouye, J.E. Tisdale, QT interval prolongation and the risk of torsades de pointes: essentials for clinicians, Curr. Med. Res. Opin. 29 (2013) 1719–1726, https://doi.org/10.1185/03007995.2013.840568.

[16] S.D. Pokorney, D.C. Yen, K.B. Campbell, N.M. Allen LaPointe, S. Sheng, L. Thomas, T.D. Bahnson, J.P. Daubert, J.P. Picini, K.P. Jackson, K.L. Thomas, S. M. Al-Khatib, Dofetilide dose reductions and discontinuations in women compared with men, Heart Rhythm. 15 (2018) 478–484, https://doi.org/10.1016/J.HRTHM.2018.01.027.

[17] D.L. Wolbrette, Risk of proarrhythmia with class III antiarrhythmic agents: sex-based differences and other issues, Am. J. Cardiol. 91 (2003) 39–44, https://doi.org/10.1016/S0002-9149(02)03378-7.

[18] O. Flórez-Vargas, A. Brass, G. Karystianis, M. Bramhall, R. Stevens, S. Cruickshank, G. Nenadic, Bias in the reporting of sex and age in biomedical research on mouse models, Elife 5 (2016), https://doi.org/10.7554/ELIFE.13615.

[19] C. Vitale, M. Fini, I. Spoletini, M. Lainscak, P. Seferovic, G.M. Rosano, Under-representation of elderly and women in clinical trials, Int. J. Cardiol. 232 (2017) 216–221, https://doi.org/10.1016/J.IJCARD.2017.01.018.

[20] C. Torp-Pedersen, M. Møller, P.E. Bloch-Thomsen, L. Køber, E. Sandøe, K. Egstrup, E. Agner, J. Carlsen, J. Videbaek, B. Marchant, A.J. Camm, Dofetilide in patients with congestive heart failure and left ventricular dysfunction. Danish investigations of arrhythmia and mortality on dofetilide study group, N. Engl. J. Med. 341 (1999) 427–428, https://doi.org/10.1056/NEJM199909163411201.

[21] L. Køber, P.E. Bloch Thomsen, M. Møller, C. Torp-Pedersen, J. Carlsen, E. Sandøe, K. Egstrup, E. Agner, J. Videbæk, B. Marchant, A.J. Camm, Effect of dofetilide in patients with recent myocardial infarction and left-ventricular dysfunction: a randomised trial, Lancet 356 (2000) 2052–2058, https://doi.org/10.1016/S0140-6736(00)03402-4.

[22] S. Singh, R.G. Zoble, L. Yellen, M.A. Brodsky, G.K. Feld, M. Berk, J. Billing, Efficacy and safety of oral dofetilide in converting to and maintaining sinus rhythm in patients with chronic atrial fibrillation or atrial flutter: the symptomatic atrial fibrillation investigative research on dofetilide (SAFIRE-D) study, Circulation 102 (2000) 2385–2390, https://doi.org/10.1161/01.CIR.102.19.2385.

[23] G.R. Mirams, Y. Cui, A. Sher, M. Fink, J. Cooper, B.M. Heath, N.C. McMahon, D. J. Gavaghan, D. Noble, Simulation of multiple ion channel block provides improved early prediction of compounds' clinical torsadogenic risk, Cardiovasc. Res. 91 (2011) 53–61, https://doi.org/10.1093/cvr/cvr044.

[24] L. Romero, J. Cano, J. Gomis-Tena, B. Trenor, F. Sanz, M. Pastor, J. Saiz, In silico QT and APD prolongation assay for early screening of drug-induced proarrhythmic risk, J. Chem. Inf. Model. 58 (2018) 867–878, https://doi.org/10.1021/acs.jcim.7b00440.

[25] J. Parikh, V. Gurev, J.J. Rice, Novel two-step classifier for torsades de pointes risk stratification from direct features, Front Pharmacol. 8 (2017) 816, https://doi.org/10.3389/fphar.2017.00816.

[26] X. Zhuang, C. Lu, PBPK modeling and simulation in drug research and development, Acta Pharm. Sin. B 6 (2016) 430, https://doi.org/10.1016/J.APSB.2016.04.004.

[27] V. Goti, A. Chaturvedula, M.J. Fossler, S. Mok, J.T. Jacob, Hospitalized patients with and without hemodialysis have markedly different vancomycin pharmacokinetics: a population pharmacokinetic model-based analysis, Ther. Drug Monit. 40 (2018) 212–221, https://doi.org/10.1097/FTD.0000000000000490.

[28] P. Liu, L. Wang, D. Han, C. Sun, X. Xue, G. Li, Acquired long QT syndrome in chronic kidney disease patients, Ren. Fail. 42 (2020) 54, https://doi.org/10.1080/0886022X.2019.1707098.

[29] O.P. Soldin, D.R. Mattison, Sex Differences in pharmacokinetics and pharmacodynamics, Clin. Pharmacokinet. 48 (2009) 143, https://doi.org/10.2165/00003088-200948030-00001.

[30] S.E. Rosenbaum, Basic Pharmacokinetics and Pharmacodynamics: An Integrated Textbook and Computer Simulations, John Wiley & Sons, 2016. https://books.google.com/books/about/Basic_Pharmacokinetics_and_Pharmacodynam.html?hl=es&id=11B4DQAAQBAJ (Accessed 14 September 2023).

[31] A. Lereclus, T. Korchia, C. Riff, F. Dayan, O. Blin, S. Benito, R. Guilhaumou, Towards precision dosing of clozapine in schizophrenia: external evaluation of population pharmacokinetic models and bayesian forecasting, Ther. Drug Monit. 44 (2022) 674–682, https://doi.org/10.1097/FTD.0000000000000987.

[32] T. O'Hara, L. Virág, A. Varró, Y. Rudy, Simulation of the undiseased human cardiac ventricular action potential: model formulation and experimental validation, PLoS Comput. Biol. 7 (2011), e1002061, https://doi.org/10.1371/journal.pcbi.1002061.

[33] S. Dutta, D. Strauss, T. Colatsky, Z. Li, Optimization of an in silico cardiac cell model for proarrhythmia risk assessment, in: 2016 Computing in Cardiology Conference (CinC), 2016, pp. 869–872, https://doi.org/10.22489/CinC.2016.253-483.

[34] E. Passini, A. Mincholé, R. Coppini, E. Cerbai, B. Rodriguez, S. Severi, A. Bueno-Orovio, Mechanisms of pro-arrhythmic abnormalities in ventricular repolarisation and anti-arrhythmic therapies in human hypertrophic cardiomyopathy, J. Mol. Cell. Cardiol. 96 (2016) 72–81, https://doi.org/10.1016/j.yjmcc.2015.09.003.

[35] M.T. Mora, J.M. Ferrero, L. Romero, B. Trenor, Sensitivity analysis revealing the effect of modulating ionic mechanisms on calcium dynamics in simulated human heart failure, PLoS ONE 12 (2017), e0187739, https://doi.org/10.1371/journal.pone.0187739.

[36] N. Gaborit, A. Varro, S.Le Bouter, V. Szuts, D. Escande, S. Nattel, S. Demolombe, Gender-related differences in ion-channel and transporter subunit expression in non-diseased human hearts, J. Mol. Cell. Cardiol. 49 (2010) 639–646, https://doi.org/10.1016/J.YJMCC.2010.06.005.

[37] P.C. Yang, C.E. Clancy, In silico prediction of sex-based differences in human susceptibility to cardiac ventricular tachyarrhythmias, Front. Physiol. 3 (2012) 360, https://doi.org/10.3389/FPHYS.2012.00360/ABSTRACT.

[38] P.C. Yang, L.L. Perissinotti, F. López-Redondo, Y. Wang, K.R. DeMarco, M.T. Jeng, I. Vorobyov, R.D. Harvey, J. Kurokawa, S.Y. Noskov, C.E. Clancy, A multiscale computational modelling approach predicts mechanisms of female sex risk in the setting of arousal-induced arrhythmias, J. Physiol. 595 (2017) 4695–4723, https://doi.org/10.1113/JP273142.

[39] A.O. Verkerk, R. Wilders, M.W. Veldkamp, W. de Geringel, J.H. Kirkels, H.L. Tan, Gender disparities in cardiac cellular electrophysiology and arrhythmia susceptibility in human failing ventricular myocytes, Int. Heart J. 46 (2005) 1105–1118, https://doi.org/10.1536/IHJ.46.1105.

[40] K.C. Chang, S. Dutta, G.R. Mirams, K.A. Beattie, J. Sheng, P.N. Tran, M. Wu, W. W. Wu, T. Colatsky, D.G. Strauss, Z. Li, Uncertainty quantification reveals the importance of data variability and experimental design considerations for in silico proarrhythmia risk assessment, Front. Physiol. 8 (2017) 917, https://doi.org/10.3389/FPHYS.2017.00917/BIBTEX.

[41] A. Lopez-Perez, R. Sebastian, M. Izquierdo, R. Ruiz, M. Bishop, J.M. Ferrero, Personalized cardiac computational models: from clinical data to simulation of infarct-related ventricular tachycardia, Front. Physiol. 10 (2019) 580, https://doi.org/10.3389/FPHYS.2019.00580/BIBTEX.

[42] E.F. Carpio, J.F. Gomez, R. Sebastian, A. Lopez-Perez, E. Castellanos, J. Almendral, J.M. Ferrero, B. Trenor, Optimization of lead placement in the right ventricle during cardiac resynchronization therapy. A simulation study, Front. Physiol. 10 (2019) 74, https://doi.org/10.3389/FPHYS.2019.00074/BIBTEX.

[43] P. Taggart, P.M. Sutton, T. Opthof, R. Coronel, R. Trimlett, W. Pugsley, P. Kallis, Inhomogeneous transmural conduction during early ischaemia in patients with coronary artery disease, J. Mol. Cell. Cardiol. 32 (2000) 621–630, https://doi.org/10.1006/JMCC.2000.1105.

[44] A. Ferrer, R. Sebastián, D. Sánchez-Quintana, J.F. Rodríguez, E.J. Godoy, L. Martínez, J. Saiz, Detailed anatomical and electrophysiological models of human atria and torso for the simulation of atrial activation, PLoS ONE 10 (2015), https://doi.org/10.1371/JOURNAL.PONE.0141573.

[45] E.F. Carpio, J.F. Gomez, J.F. Rodríguez-Matas, B. Trenor, J.M. Ferrero, Analysis of vulnerability to reentry in acute myocardial ischemia using a realistic human heart model, Comput. Biol. Med. 141 (2022), 105038, https://doi.org/10.1016/J.COMPBIOMED.2021.105038.

[46] P. Stewart, O.v. Aslanidi, D. Noble, P.J. Noble, M.R. Boyett, H. Zhang, Mathematical models of the electrical action potential of Purkinje fibre cells, Philos. Trans. R. Soc. A Math. Phys. Eng. Sci. 367 (2009) 2225–2255, https://doi.org/10.1098/RSTA.2008.0283.

[47] E.A. Heidenreich, J.M. Ferrero, M. Doblaré, J.F. Rodríguez, Adaptive macro finite elements for the numerical solution of monodomain equations in cardiac electrophysiology, Ann. Biomed. Eng. 38 (2010) 2331–2345, https://doi.org/10.1007/S10439-010-9997-2.

[48] L. Phillips, T.H. Grasela, J.R. Agnew, E.A. Ludwig, G.A. Thompson, A population pharmacokinetic-pharmacodynamic analysis and model validation of azimilide, Clin. Pharmacol. Ther. 70 (2001) 370–383, https://doi.org/10.1016/S0009-9236(01)56650-3.

[49] Y. Preechagoon, B. Charles, V. Piotrovskij, T. Donovan, A. Van Peer, Population pharmacokinetics of enterally administered cisapride in young infants with gastro-oesophageal reflux disease, Br. J. Clin. Pharmacol. 48 (1999) 688–693, https://doi.org/10.1046/J.1365-2125.1999.00068.X.

[50] Résumé des Caractéristiques du Produit, (n.d.). http://agence-prd.ansm.sante.fr/php/ecodex/rcp/R0122266.htm (accessed September 15, 2023).

[51] V. Arora, M. Spino, Cisapride: a novel gastroprokinetic drug, Can. J. Hosp. Pharm. 44 (1991), https://doi.org/10.4212/CJHP.V44I4.2754.

[52] M. Jerling, Y. Merlé, F. Mentré, A. Mallet, Population pharmacokinetics of clozapine evaluated with the nonparametric maximum likelihood method, Br. J. Clin. Pharmacol. 44 (1997) 447–453, https://doi.org/10.1046/J.1365-2125.1997.T01-1-00606.X.

[53] C.N. Verme, T.M. Ludden, W.A. Clementi, S.C. Harris, Pharmacokinetics of quinidine in male patients: a population analysis, Clin. Pharmacokinet. 22 (1992) 468–480, https://doi.org/10.2165/00003088-199222060-00005/METRICS.

[54] L.K. Foo, S.B. Duffull, L. Calver, J. Schneider, G.K. Isbister, Population pharmacokinetics of intramuscular droperidol in acutely agitated patients, Br. J. Clin. Pharmacol. 82 (2016) 1550–1556, https://doi.org/10.1111/BCP.13093.

[55] G. Nucci, R. Gomeni, Population pharmacokinetic modelling of pimozide and its relation to CYP2D6 genotype, in: Annual Meeting of Population Approach Group in Europe, 2007. https://www.page-meeting.org/pdf_assets/2013-Pimozide_PopPK.pdf. Accessed 15 September 2023.

[56] A. Thyssen, A. Vermeulen, E. Fuseau, M.A. Fabre, E. Mannaert, Population pharmacokinetics of oral risperidone in children, adolescents and adults with psychiatric disorders, Clin. Pharmacokinet. 49 (2010) 465–478, https://doi.org/10.2165/11531730-000000000-00000.

[57] Résumé des caractéristiques du produit - ZECLAR 500 mg, comprimé pelliculé - Base de données publique des médicaments, (n.d.). https://base-donnees-publique.medicaments.gouv.fr/affichageDoc.php?specid=67997205&typedoc=R#RcpPropPharmacocinetiques (accessed 15 September 2023, 2023).

[58] L.L. Brunton, R. Hilal-Dandan, B.C. Knollmann, Goodman & Gilman's: The Pharmacological Basis of Therapeutics, 13th ed., Mc Graw Hill, 2018. https://accessmedicine.mhmedical.com/book.aspx?bookID=2189. Accessed 15 September 2023.

[59] Résumé des caractéristiques du produit - RYTHMODAN 250 mg A LIBERATION PROLONGEE, comprimé enrobé - Base de données publique des médicaments, (n.d.). https://base-donnees-publique.medicaments.gouv.fr/affichageDoc.php?specid=69235837&typedoc=R#RcpPosoAdmin (accessed 15 September 2023, 2023).

[60] Résumé des caractéristiques du produit - RYTHMODAN 100 mg, gélule - Base de données publique des médicaments, (n.d.). https://base-donnees-publique.medicaments.gouv.fr/affichageDoc.php?specid=63063487&typedoc=R#RcpPosoAdmin (accessed 15 September 2023, 2023).

[61] Pfizer Laboratories Div Pfizer Inc, TIKOSYN-dofetilide capsule, (2023). https://labeling.pfizer.com/showlabeling.aspx?id=639 (accessed 7 February 2023).

[62] Résumé des caractéristiques du produit - ONDANSETRON ARROW 8 mg, comprimé pelliculé - Base de données publique des médicaments, (n.d.). https://base-donnees-publique.medicaments.gouv.fr/affichageDoc.php?specid=63782187&typedoc=R#RcpPropPharmacocinetiques (accessed 15 September 2023, 2023).

[63] S.A. Helmy, H.M. El Bedaiwy, Pharmacokinetics and comparative bioavailability of domperidone suspension and tablet formulations in healthy adult subjects, Clin. Pharmacol. Drug Dev. 3 (2014) 126–131, https://doi.org/10.1002/CPDD.43.

[64] P. Martin, S. Oliver, S.J. Kennedy, E. Partridge, M. Hutchison, D. Clarke, P. Giles, Pharmacokinetics of vandetanib: three phase I studies in healthy subjects, Clin. Ther. 34 (2012) 221–237, https://doi.org/10.1016/J.CLINTHERA.2011.11.011.

[65] T. Humphrey, M.R. Davids, M.Y. Chothia, R. Pecoits-Filho, C. Pollock, G. James, How common is hyperkalaemia? A systematic review and meta-analysis of the prevalence and incidence of hyperkalaemia reported in observational studies, Clin. Kidney J. 15 (2022) 727–737, https://doi.org/10.1093/CKJ/SFAB243.

[66] R.P.M. te Dorsthorst, J. Hendrikse, M.T. Vervoorn, V.Y.H. van Weperen, M.A. G. van der Heyden, Review of case reports on hyperkalemia induced by dietary intake: not restricted to chronic kidney disease patients, Eur. J. Clin. Nutr. 73 (1) (2018) 38–45, https://doi.org/10.1038/s41430-018-0154-6.

[67] L. Kuepfer, C. Niederalt, T. Wendl, J.F. Schlender, S. Willmann, J. Lippert, M. Block, T. Eissing, D. Teutonico, Applied concepts in PBPK modeling: how to build a PBPK/PD model, CPT Pharmacometrics Syst. Pharmacol. 5 (2016) 516–531, https://doi.org/10.1002/PSP4.12134.

[68] R.L. Lalonde, J.A. Wagner, Drug development perspective on pharmacokinetic studies of new drugs in patients with renal impairment, Clin. Pharmacol. Ther. 86 (2009) 557–561, https://doi.org/10.1038/CLPT.2009.182.

[69] S. Polak, In vitro to human in vivo translation - pharmacokinetics and pharmacodynamics of quinidine, ALTEX 30 (2013) 309–318, https://doi.org/10.14573/ALTEX.2013.3.309.

[70] M. Varshneya, I. Irurzun-Arana, C. Campana, R. Dariolli, A. Gutierrez, T. K. Pullinger, E.A. Sobie, Investigational treatments for COVID-19 may increase ventricular arrhythmia risk through drug interactions, CPT Pharmacometrics Syst. Pharmacol. 10 (2021) 100–107, https://doi.org/10.1002/PSP4.12573.

[71] B. Wiśniowska, M. Holbrook, C. Pollard, S. Polak, Utilization of mechanistic modelling and simulation to analyse fenspiride proarrhythmic potency – role of physiological and other non-drug related parameters, J. Clin. Pharm. Ther. 47 (2022) 2152–2161, https://doi.org/10.1111/JCPT.13762.

[72] H. Zhou, Z. Zhang, L. Zhu, P. Li, S. Hong, L. Liu, X. Liu, Prediction of drug pro-arrhythmic cardiotoxicity using a semi-physiologically based pharmacokinetic model linked to cardiac ionic currents inhibition, Toxicol. Appl. Pharmacol. 457 (2022), https://doi.org/10.1016/J.TAAP.2022.116312.

[73] N. Gaborit, S.Le Bouter, V. Szuts, A. Varro, D. Escande, S. Nattel, S. Demolombe, Regional and tissue specific transcript signatures of ion channel genes in the non-diseased human heart, J. Physiol. 582 (2007) 675–693, https://doi.org/10.1113/JPHYSIOL.2006.126714.

[74] J. Vicente, L. Johannesen, L. Galeotti, D.G. Strauss, Mechanisms of sex and age differences in ventricular repolarization in humans, Am. Heart. J. 168 (2014) 749–756, https://doi.org/10.1016/J.AHJ.2014.07.010, e3.

[75] B. Surawicz, S.R. Parikh, Differences between ventricular repolarization in men and women: description, mechanism and implications, Ann. Noninvasive Electrocardiol. 8 (2003) 333, https://doi.org/10.1046/J.1542-474X.2003.08411.X.

[76] P.M. Rautaharju, S.H. Zhou, S. Wong, H.P. Calhoun, G.S. Berenson, R. Prineas, A. Davignon, Sex differences in the evolution of the electrocardiographic QT interval with age, Can. J. Cardiol. 8 (7) (1992) 690–695. PMID: 1422988.

[77] O.J. Britton, N. Abi-Gerges, G. Page, A. Ghetti, P.E. Miller, B. Rodriguez, Quantitative comparison of effects of dofetilide, sotalol, quinidine, and verapamil between human ex vivo trabeculae and in silico ventricular models incorporating inter-individual action potential variability, Front. Physiol. 8 (2017) 597, https://doi.org/10.3389/fphys.2017.00597.

[78] K. Blinova, Q. Dang, D. Millard, G. Smith, J. Pierson, L. Guo, M. Brock, H.R. Lu, U. Kraushaar, H. Zeng, H. Shi, X. Zhang, K. Sawada, T. Osada, Y. Kanda, Y. Sekino, L. Pang, T.K. Feaster, R. Kettenhofen, N. Stockbridge, D.G. Strauss, G. Gintant, International multisite study of human-induced pluripotent stem cell-derived cardiomyocytes for drug proarrhythmic potential assessment, Cell Rep. 24 (2018) 3582–3592, https://doi.org/10.1016/J.CELREP.2018.08.079.

[79] H. Sutanto, L. Laudy, M. Clerx, D. Dobrev, H.J.G.M. Crijns, J. Heijman, Maastricht antiarrhythmic drug evaluator (MANTA): a computational tool for better understanding of antiarrhythmic drugs, Pharmacol. Res. 148 (2019), https://doi.org/10.1016/J.PHRS.2019.104444.

[80] P. Gluais, M. Bastide, J. Caron, M. Adamantidis, Comparative effects of clarithromycin on action potential and ionic currents from rabbit isolated atrial and ventricular myocytes, J. Cardiovasc. Pharmacol. 41 (2003) 506–517, https://doi.org/10.1097/00005344-200304000-00002.

[81] X. Chen, J.S. Cordes, J.A. Bradley, Z. Sun, J. Zhou, Use of arterially perfused rabbit ventricular wedge in predicting arrhythmogenic potentials of drugs, J. Pharmacol. Toxicol. Methods 54 (2006) 261–272, https://doi.org/10.1016/J.VASCN.2006.02.005.

[82] P. Gluais, M. Bastide, J. Caron, M. Adamantidis, Risperidone prolongs cardiac action potential through reduction of K+ currents in rabbit myocytes, Eur. J. Pharmacol. 444 (2002) 123–132, https://doi.org/10.1016/S0014-2999(02)01626-6.

[83] M. RR, F. BS, S. RT, M. MD, L. MH, Female gender as a risk factor for torsades de pointes associated with cardiovascular drugs, JAMA 270 (1993) 2590–2597, https://doi.org/10.1001/JAMA.270.21.2590.

[84] A.F. James, S.C.M. Choisy, J.C. Hancox, Recent advances in understanding sex differences in cardiac repolarization, Prog. Biophys. Mol. Biol. 94 (2007) 265–319, https://doi.org/10.1016/J.PBIOMOLBIO.2005.05.010.

[85] A. Fogli Iseppe, H. Ni, S. Zhu, X. Zhang, R. Coppini, P.C. Yang, U. Srivatsa, C. E. Clancy, A.G. Edwards, S. Morotti, E. Grandi, Sex-specific classification of drug-induced torsade de pointes susceptibility using cardiac simulations and machine learning, Clin. Pharmacol. Ther. 110 (2021) 380–391, https://doi.org/10.1002/CPT.2240.

[86] M. Peirlinck, F. Sahli Costabal, E. Kuhl, Sex differences in drug-induced arrhythmogenesis, Front. Physiol. 12 (2021) 1245, https://doi.org/10.3389/FPHYS.2021.708435/BIBTEX.

[87] H. Sutanto, D.M. Hertanto, H. Susilo, C.D.K. Wungu, Grapefruit flavonoid naringenin sex-dependently modulates action potential in an in silico human ventricular cardiomyocyte model, Antioxidants (Basel) 11 (2022), https://doi.org/10.3390/ANTIOX11091672.

[88] N. El-Sherif, G. Turitto, M. Boutjdir, Acquired long QT syndrome and electrophysiology of torsade de pointes, Arrhythm. Electrophysiol. Rev. 8 (2019) 122–130, https://doi.org/10.15420/AER.2019.8.3.
[89] D. Shaffer, S. Singer, J. Korvick, P. Honig, Concomitant risk factors in reports of torsades de pointes associated with macrolide use: review of the United States food and drug administration adverse event reporting system, Clin. Infect. Dis. 35 (2002) 197–200, https://doi.org/10.1086/340861.
[90] S. Genovesi, E. Nava, C. Bartolucci, S. Severi, A. Vincenti, G. Contaldo, G. Bigatti, D. Ciurlino, S.V. Bertoli, Acute effect of a peritoneal dialysis exchange on electrolyte concentration and QT interval in uraemic patients, Clin. Exp. Nephrol. 23 (2019) 1315–1322, https://doi.org/10.1007/S10157-019-01773-Y.
[91] L. Johannesen, J. Vicente, J.W. Mason, C. Sanabria, K. Waite-Labott, M. Hong, P. Guo, J. Lin, J.S. Sørensen, L. Galeotti, J. Florian, M. Ugander, N. Stockbridge, D.G. Strauss, Differentiating drug-induced multichannel block on the electrocardiogram: randomized study of dofetilide, quinidine, ranolazine, and verapamil, Clin. Pharmacol. Ther. 96 (2014) 549–558, https://doi.org/10.1038/CLPT.2014.155.
[92] F.Le Coz, C. Funck-Brentano, T. Morell, M.M. Ghadanfar, P. Jaillon, Pharmacokinetic and pharmacodynamic modeling of the effects of oral and intravenous administrations of dofetilide on ventricular repolarization, Clin. Pharmacol. Ther. 57 (1995) 533–542, https://doi.org/10.1016/0009-9236(95)90038-1.
[93] R.C. Elkins, M.R. Davies, S.J. Brough, D.J. Gavaghan, Y. Cui, N. Abi-Gerges, G. R. Mirams, Variability in high-throughput ion-channel screening data and consequences for cardiac safety assessment, J. Pharmacol. Toxicol. Methods 68 (2013) 112–122, https://doi.org/10.1016/J.VASCN.2013.04.007.
[94] S. Polak, B. Wiśniowska, J. Brandys, Collation, assessment and analysis of literature in vitro data on hERG receptor blocking potency for subsequent modeling of drugs' cardiotoxic properties, J. Appl. Toxicol. 29 (2009) 183–206, https://doi.org/10.1002/jat.1395.
[95] J. Gomis-Tena, B.M. Brown, J. Cano, B. Trenor, P.-C. Yang, J. Saiz, C.E. Clancy, L. Romero, When does the IC50 accurately assess the blocking potency of a drug? J. Chem. Inf. Model. 2020 (2020) 1779–1790, https://doi.org/10.1021/acs.jcim.9b01085.
[96] A. Dasgupta, Usefulness of monitoring free (unbound) concentrations of therapeutic drugs in patient management, Clin. Chim. Acta 377 (2007) 1–13, https://doi.org/10.1016/J.CCA.2006.08.026.
[97] F. Zhang, J. Xue, J. Shao, L. Jia, Compilation of 222 drugs' plasma protein binding data and guidance for study designs, Drug Discov. Today 17 (2012) 475–485, https://doi.org/10.1016/J.DRUDIS.2011.12.018.
[98] W.C. Dong, J.L. Guo, X.K. Wu, M.Q. Zhao, H.R. Li, Z.Q. Zhang, Y. Jiang, Relationship between the free and total methotrexate plasma concentration in children and application to predict the toxicity of HD-MTX, Front. Pharmacol. 12 (2021), 636975, https://doi.org/10.3389/FPHAR.2021.636975/BIBTEX.
[99] S.A. Adelusi, L.A. Salako, Tissue and blood concentrations of chloroquine following chronic administration in the rat, J. Pharm. Pharmacol. 34 (1982) 733–735, https://doi.org/10.1111/J.2042-7158.1982.TB06211.X.
[100] S. Polak, Z. Tylutki, M. Holbrook, B. Wiśniowska, Better prediction of the local concentration–effect relationship: the role of physiologically based pharmacokinetics and quantitative systems pharmacology and toxicology in the evolution of model-informed drug discovery and development, Drug Discov. Today 24 (2019) 1344–1354, https://doi.org/10.1016/J.DRUDIS.2019.05.016.
[101] S. Nattel, Y. Frelin, N. Gaborit, C. Louault, S. Demolombe, Ion-channel mRNA-expression profiling: insights into cardiac remodeling and arrhythmic substrates, J. Mol. Cell. Cardiol. 48 (2010) 96–105, https://doi.org/10.1016/J.YJMCC.2009.07.016.
[102] J. Walmsley, J.F. Rodriguez, G.R. Mirams, K. Burrage, I.R. Efimov, B. Rodriguez, mRNA expression levels in failing human hearts predict cellular electrophysiological remodeling: a population-based simulation study, PLoS ONE 8 (2013), https://doi.org/10.1371/JOURNAL.PONE.0056359.
[103] B. Danielsson, J. Collin, A. Nyman, A. Bergendal, N. Borg, M. State, L. Bergfeldt, J. Fastbom, Drug use and torsades de pointes cardiac arrhythmias in Sweden: a nationwide register-based cohort study, BMJ Open 10 (2020), https://doi.org/10.1136/BMJOPEN-2019-034560.